Reference:
Churchman, G.J., Pasbakhsh, P., Lowe, D.J., Theng, B.K.G. 2016. Unique but diverse: some observations on the formation, structure, and morphology of halloysite. *Clay Minerals* 51, 395-416.

Unique but diverse: some observations on the formation, structure and morphology of halloysite.

G.J. CHURCHMAN[1*], P. PASBAKHSH[2], D.J. LOWE[3] AND B.K.G. THENG[4]

[1]School of Agriculture, Food and Wine, University of Adelaide, Adelaide 5005, Australia, [2]School of Engineering, Monash University, Selangor 47500, Malaysia, [3]School of Science, Faculty of Science and Engineering, University of Waikato, Hamilton 3240, New Zealand, [4]Landcare Research, Palmerston North 4442, New Zealand

Submitted: 4 November 2015. Revised: 11 June 2016. Guest Editor: Steve Hillier.

ABSTRACT: New insights from the recent literature are summarised and new data presented concerning the formation, structure and morphology of halloysite. Halloysite formation by weathering always requires the presence of water. Where substantial drying occurs, kaolinite is formed instead. Halloysite formation is favoured by a low pH. The octahedral sheet is positively charged at pH < ~8, whereas the tetrahedral sheet is negatively charged at pH > ~2. The opposing sheet charge would facilitate interlayer uptake of H_2O molecules. When halloysite intercalates certain polar organic molecules, additional (hkl) reflections appear in the X-ray diffractogram, suggesting layer re-arrangement which, however, is dissimilar to that in kaolinite. Associated oxides and oxyhydroxides of Fe and Mn may limit the growth of halloysite particles as does incorporation of Fe into the structure. Particles of different shape and iron content may occur within a given sample of halloysite.

KEYWORDS: Water, pH, Iron, Particle size, Morphology, Organic complexes, 2-layer structure

* E-mail: jock.churchman@adelaide.edu.au

Since halloysite was first described by Berthier (1826), the clay mineral has attracted a great deal of attention and interest. Halloysite has the same chemical composition as kaolinite but, unlike kaolinite, can intercalate up to two molecules of H_2O per $Al_2Si_2O_5(OH)_4$ unit cell (Hofmann *et al*., 1934; Mehmel, 1935; MacEwan, 1947; Churchman & Carr, 1975). Advanced instrumental techniques have revealed interesting and surprising features about the particle morphology and composition of halloysite.

A surprising feature, observed by electron microscopy, is that halloysite particles are commonly fibrous (Alexander *et al*., 1943) whereas kaolinite is platy with a hexagonal outline. Furthermore, halloysite samples from different localities can adopt a variety of particle shapes, including spheroidal, platy, and prismatic, in addition to being fibrous or tubular (Joussein *et al*., 2005; Churchman, 2015; Moon et al., 2015).

Halloysites are also distinguishable from kaolinites by their infrared and Raman spectra, thermal analyses patterns, and reactivity toward ionic and polar organic compounds. In combination with X-ray diffraction (XRD), these measurements have led to the suggestion that halloysite is a highly disordered form of kaolin (Churchman & Carr, 1975; Joussein *et al*., 2005; Churchman, 2015).

Aspects of the identity of halloysite remain controversial, even after many reviews and critical articles (MacEwan, 1947; Churchman & Carr, 1975; Bailey, 1990; Joussein *et al*., 2005; Churchman, 2015; Guggenheim, 2015). There are still fundamental questions about the structure of halloysite, with implications for its nomenclature and identification.

Since its discovery by Berthier (1826), halloysite has usually been described and defined in terms of its differences from kaolinite, the essential difference being the presence of

This is a 'pre-published' version of a paper accepted for publication in Clay Minerals.
This version may be changed during the production process.
The DOI, which may be used for citation purposes, but which will not be active until the version of record is published, is 10.1180/claymin.2016.051.3.14

interlayer H_2O in halloysite. This feature has led Churchman & Carr (1975) to define halloysites as "those minerals with a kaolin layer structure which either contain interlayer water in their natural state, or for which there is unequivocal evidence of their formation by dehydration from kaolin minerals containing interlayer water". Strictly speaking, the interlayer water in halloysite should be denoted as "H_2O" or "H_2O molecules" (Clay Minerals Society, 2015).

This definition is consistent with the formamide test for dehydrated halloysite, giving an XRD pattern that is difficult to distinguish from that of a highly-disordered kaolinite (Churchman *et al*., 1984). Thus, when formamide is added to a sample containing halloysite that has lost interlayer H_2O, the compound rapidly enters the interlayer space, expanding it to a similar extent as H_2O. Although kaolinite can also intercalate formamide, the process requires several hours. Furthermore, halloysites expand more readily than kaolinites on intercalation of polar molecules other than formamide (Theng *et al*., 1984; Churchman, 1990, 2015), reflecting the 'priming' effect of H_2O in expanding the interlayer space. Although the formamide test is widely used and generally accepted (Christidis, 2013; Lagaly *et al*., 2013; Środoń, 2013), it fails with samples that have been pre-heated (Churchman *et al*., 1984). The test may also fail with halloysites that form during periods of high temperature and dehydration (Churchman & Gilkes, 1989; Janik & Keeling, 1993). The formamide test is also ineffective with K^+-selective halloysite samples (Takahashi *et al*., 1993, 2001), apparently because of interstratification of 2:1 aluminosilicate layers (Joussein *et al*., 2005, 2007)**.** Nonetheless, a positive formamide test would show the presence of halloysite.

Probably the most controversial contribution to the literature on halloysite in the past few decades has been that of Bailey (1990) who proposed that H_2O is attracted to, and retained in, the interlayer of halloysite because its layer charge is greater (more negative) than that of kaolinite. Hydrated cations then enter the interlayer space to balance the negative layer charge. Bailey (1990) has further postulated that the excess negative charge in halloysite (over that in kaolinite) arises from a small, but significant, substitution of Al^{3+} for Si^{4+} in the tetrahedral sheet. This postulate, however, is inconsistent with ^{27}Al NMR analyses by Newman *et al*. (1994) indicating that halloysites have similar Al(IV) contents to standard kaolinite.

Here we summarise the most recent information on the formation, structure, and morphology of halloysites to augment or amend that given in the reviews by Joussein *et al*. (2005) and Guggenheim (2015). In addition, some new data are presented.

FORMATION

Like kaolinite, halloysite is formed as an alteration product of weathering or hydrothermal activity. In general, kaolinisation is favoured by warm, wet, and mildly acidic conditions when K^+, Na^+, Ca^{2+}, and Mg^{2+} ions can flow through the solution, and some loss of SiO_2 can occur through leaching (Galán, 2006; Keeling, 2015). At the "type" locality of halloysite (Berthier, 1826), the mineral formed from sulphide oxidation leading to acidified groundwater passing through sandy sediments overlying limestone. Halloysite formed where Al, released by the acidified groundwater, combined with Si, and was precipitated on meeting a pH gradient. (Dupuis & Ertus, 1995; Keeling, 2015). The extensive deposits of

This is a 'pre-published' version of a paper accepted for publication in Clay Minerals.
This version may be changed during the production process.
The DOI, which may be used for citation purposes, but which will not be active until the version of record is published, is 10.1180/claymin.2016.051.3.14

halloysite at Carlsbad Cavern, New Mexico (Polyak & Güven, 1996), Djebel Debbagh, Algeria (Renac & Assassi, 2009) and Camel playa lake, South Australia (Keeling *et al*., 2010), formed through a similar process. In the South Australian case, halloysite formation was promoted by acidified groundwater discharged from underlying lignite sands beneath a limestone cover.

The fluids responsible for mineral alteration may be hydrothermal, as in occurrences of halloysite in Japan, Mexico, Turkey, Thailand, and China as well as of the commercial Dragon halloysite mine in Utah (Keeling, 2015). The world's dominant source of halloysite, at Matauri Bay in northern New Zealand, was thought to have been formed by hydrothermal activity, in combination with weathering of (rhyolitic/basaltic) volcanic deposits. Brathwaite *et al*. (2012, 2014), however, showed that weathering was the primary agent of alteration, as was the case for halloysites in Poland, Brazil, and Argentina (Keeling, 2015). The following discussion concerns recent investigations of the formation of halloysite by weathering.

Halloysite occurs in surface horizons of soils world-wide, often through weathering of volcanic parent materials (e.g., Fieldes & Swindale, 1954; Fieldes, 1968; Tazaki, 1979; Parfitt *et al.*, 1983; Stevens & Vucetich, 1985; Lowe, 1986; Mizota & van Reeuwijk, 1989; Lowe & Percival, 1993; Torn *et al*., 1997; Churchman, 2000; Rasmussen *et al*., 2007; Churchman & Lowe, 2012). Halloysite also occurs within weathering profiles formed on many other rock types (Churchman, 2000; Joussein *et al*., 2005). These profiles have formed in a variety of climates, including tropical (e.g., Eswaran & Yeow, 1976; Eswaran & Wong, 1978), temperate (e.g., Calvert *et al*., 1980; Churchman, 1990), and Mediterranean or xeric (e.g., Churchman & Gilkes, 1989; Takahashi *et al.*, 2001; Singer *et al.*, 2004; Churchman & Lowe, 2012). In many profiles, there is substantial halloysite at depth but little or none at the

This is a 'pre-published' version of a paper accepted for publication in Clay Minerals.
This version may be changed during the production process.
The DOI, which may be used for citation purposes, but which will not be active until the version of record is published, is 10.1180/claymin.2016.051.3.14

surface of the corresponding soils. Commonly, halloysite is replaced by kaolinite as the dominant clay mineral towards the top of weathering profiles. Not many studies have quantified the mineralogical changes with depth, but an example is shown in Fig. 1.

(Insert Fig. 1 about here)

In the profile on dolerite, described by Churchman & Gilkes (1989) (Fig. 1a, b), only halloysite among kaolin minerals appears at the lowest depth sampled (in saprolite). A substantial proportion of halloysite is also found in the sample to 4.5 m depth, within the middle to upper part of the 'mottled zone'. Kaolinite, by contrast, occurs in samples from 7.5 m depth, within the pallid zone, up into the highly laterised surface of the profile. The concentration of kaolinite gradually diminishes from 3.5 m, at the top of the mottled zone, to the surface. Of the other secondary minerals in these two profiles, gibbsite occurs throughout the profile but, together with kaolinite and halloysite, is displaced as the dominant secondary mineral by boehmite at the surface (Churchman & Gilkes, 1989). In a deeply weathered profile under a tropical climate (Eswaran & Wong, 1978), halloysite decreases gradually from ~50% (presumably of the whole sample) at about midway in the 'weathering rock' layer at >15 m, to ~5% at the surface, in the A horizon of the 'pedological profile'. By contrast, kaolinite does not appear until the top of the 'pallid zone' at ~10 m, from where it shows a steady increase to ~20% at or near the surface of the pedological (soil) profile. In the profile studied by Eswaran & Wong (1978), considerable gibbsite persists throughout the profile down into the pallid zone.

More relevant to the formation of either halloysite or kaolinite is the appearance of goethite in both profiles, from the surface down into the mottled zone in each case. This finding indicates that oxidation has occurred as far down as the mottled zone, implying

seasonal drying with depth into this zone. Halloysite apparently forms first in each case, with kaolinite forming in addition to, or else following dissolution of, the halloysite. Little, if any, halloysite, however, is found alongside goethite, whereas the formation of kaolinite is usually favoured over that of halloysite in zones of the profiles where intense seasonal drying has occurred. Nonetheless, halloysite may form and persist where drying is weak. Thus 7 Å-halloysite, rather than kaolinite, is formed in volcanic deposits or soils where some dehydration occurs (e.g., Singer *et al*., 2004; Lowe, 1986). Lowe (1986) found that 7 Å-halloysite predominated in the surface horizons of a soil developed on weathered tephra in northern New Zealand that had been subjected to common, but mild, seasonal drying whereas 10 Å-halloysite occurred in deeper horizons that were less affected by such dehydration. An intermediate zone of halloysite with XRD peaks between 10 and 7 Å occurred between upper and lower subsoil horizons (Lowe & Nelson, 1994; Churchman & Lowe, 2012).

In comparing one zone of weathering across different sites in Hong Kong, Churchman *et al.* (2010) found different occurrences of saprolites, formed under the same climatic conditions. Each of these produced veins comprising layers of infill largely containing neo-formed kaolin minerals, either halloysite or kaolinite, or both species of minerals together. Occurrences of kaolinite were accompanied by evidence of oxidation, and hence substantial drying. Neo-formed halloysite occurred in the absence of oxidised products, indicating the need for water to exist on a more or less continuous basis for halloysite to form and persist.

Fig. 2 shows white veins of infill rich in kaolin minerals, occurring in granite (Fig. 2a) and volcanic tuff (Fig. 2b). In the former instance, the veins do not contain clear visual evidence for either iron or manganese oxide. By contrast, the veins in tuff are both flanked and

streaked throughout by black Mn oxide mottles, indicative of oxidation and drying. The infill in granite contains long halloysite tubes, often parallel to one another and occurring in bunches (Fig. 2c), whereas that in tuff (Fig. 2d) contains well-formed kaolinite plates. Halloysite formed and persisted where the saprolite remained moist, as indicated by a lack of oxides, whereas kaolinite formed under otherwise similar climatic conditions but where drying occurred, leading to the formation of oxides.

Similarly, thick sequences of 10 Å-halloysite-dominated soil materials formed from weathered rhyolitic (siliceous) tephras and volcaniclastic deposits. Dating from ~0.93 Ma in the Bay of Plenty region, northern New Zealand, the deposits have high natural water contents – near permanent saturation – and low permeability. The pore water in this locally wet environment is rich in Si, derived largely from dissolution of volcanic glass shards and plagioclase. These conditions are ideal for the formation of halloysite rather than allophane (Moon *et al*., 2015). The soil materials may contain ≤ 5 % of dispersed MnO_2 redox concentrations, generally small masses or concretions, indicative of intermittent drying (Moon *et al.*, 2015). Drying, however, is only short-termed because prolonged dehydration would lead to kaolinite (which is not present) being formed (Papoulis *et al*., 2004; Churchman *et al*., 2010).

Our investigation of depth profiles, saprolites, and weathered volcanic deposits, under different moisture regimes, indicate that halloysite formation is favoured by the continuous presence of water.

As already noted, halloysite differs from other members of the kaolin sub group (kaolinite, dickite, nacrite), in having interlayer H_2O at the time of formation. Why and how halloysite intercalates water molecules, however, is as yet unclear. Bailey's (1990) proposal, described

above, has been discredited as a general explanation for all halloysites. Quasi-elastic scattering analysis by Bordallo *et al*. (2008), for example, indicates that no exchangeable cations are associated with interlayer H_2O in halloysite. The conditions under which halloysites form in nature may provide a clue to the presence of interlayer H_2O as do situations where halloysites are not formed when most conditions suitable for their formation appear to be present.

Several studies in North Island, New Zealand (Parfitt *et al*., 1983, 1984; Parfitt & Wilson, 1985; Churchman & Lowe, 2012), have shown that the weathering of rhyolitic or andesitic volcanic ash produces either allophane or halloysite, depending mainly on the moisture regime. Halloysite is formed where rainfall is relatively low (< ~1200 mm/year), whereas allophane is found under wetter conditions (> ~1600 mm/year) (Parfitt *et al*., 1983; Lowe, 1986). In Hawaii on basaltic ash, on the other hand, the rainfall transition for the formation of allophane and halloysite is considerably lower, ~600 mm/year (Parfitt, 1990), because basalts compositionally contain less silica ($\leq$ ~50% SiO_2) than andesites (~ 50–70% SiO_2) or rhyolites ($\geq$ ~70% SiO_2), and also more alumina (e.g., Churchman & Lowe, 2012). More important than rainfall, therefore, is the concentration of Si in the soil solution which, in turn, is controlled by the rate of leaching of the parent volcanic ash, its composition, and its drainage (e.g., Ugolini & Dahlgren, 2002; Churchman & Lowe, 2012). A threshold of about 250 mm leaching marks the transition from conditions favouring halloysite formation to those favouring allophane. In other words, > ~250 mm throughput of leachate results in allophane, whereas $\leq$ ~200 mm gives rise to halloysite (Parfitt *et al*., 1984; Lowe, 1995).

As in North Island, New Zealand, volcanic activity occurred in southeastern South Australia during the Pleistocene and Holocene (Sheard, 1990; Lowe & Palmer, 2005; van Otterloo *et*

This is a 'pre-published' version of a paper accepted for publication in Clay Minerals.
This version may be changed during the production process.
The DOI, which may be used for citation purposes, but which will not be active until the version of record is published, is 10.1180/claymin.2016.051.3.14

al., 2013). The youngest of the volcanoes in this province comprise two isolated basaltic eruption centres at Mounts Gambier and Schank. These near-contemporaneous centres are about 10 km apart and are between ~5,500 and 4,300 years old (Barbetti & Sheard, 1981; Smith & Prescott, 1987; Robertson *et al*., 1996; Gouramanis *et al*., 2010; Murray-Wallace, 2011). Soils formed from the basaltic scoria (cinders), lapilli, and ash spread about 10−12 km from each source were studied at ten sites: six near Mount Gambier, three near Mount Schank, and one at an intermediate site (Lowe & Palmer, 2005; Takesako *et al*., 2010).The mean annual precipitation (MAP) of ~700 mm is slightly less than that (~800−1200 mm) which gives rise to soils in parts of North Island, New Zealand, where halloysite is the dominant clay mineral (Parfitt *et al*.,1984), and about the same as the MAP for halloysite-bearing soils in Hawaii (Parfitt *et al*., 1988; Parfitt, 1990). In the case of the North Island soils, rain falls almost evenly throughout the year under a udic moisture regime in many areas (and water moves entirely through the soil profile in most years), but less rain falls during persistent dry summers in eastern areas under an ustic moisture regime (in which the profile remains moist in some parts for at least six months in most years) (Parfitt, 1990; Soil Survey Staff, 2014). By contrast, the soil moisture regime for the South Australian soils is xeric, where winters are moist and cool and summers are very dry and warm (and the profile remains moist for only a few months in most years) (Lowe & Palmer, 2005; Soil Survey Staff, 2014).

Hence in the South Australian soils the flow of water through the upper horizons is ~280 mm/year, typically for ~3 to 10 weeks during winter or early spring (Lowe & Palmer, 2005), similar to the upper threshold for halloysite formation in New Zealand. There is considerably less flow through the lower horizons in the South Australian soils, ~100 mm/year (Allison &

Hughes, 1978), which should favour halloysite formation. Peaks near 7 Å for clays from many of the soil samples were observed but the basal spacing did not expand beyond ~7 Å when formamide was applied (Lowe & Palmer, 2005), indicating the absence of halloysite (Churchman *et al*., 1984).

Because basaltic parent materials are relatively low in SiO_2 (noted above) and enriched in Al_2O_3, Si concentrations in the Mount Gambier/Schank soils might be expected to be relatively low even if kinetic factors favour halloysite formation (cf. Ziegler *et al*., 2003). However, fragmental basaltic glass dissolves readily to release Si. Some SiO_2 may also derive from siliceous marine sponge spicules that occur within the antecedent limestones incorporated as xenoliths within the basaltic eruptives. Common crystals of olivine (which weathers rapidly), titanaugite, and labradorite can also serve as potential sources of Si (Sheard *et al.*, 1993; Lowe *et al.*, 1996; Lowe & Palmer, 2005). In addition, these soils contain kaolinite and illite, accompanied sometimes by a smectitic phase, including interstratified kaolinite-smectite and/or illite-smectite, as well as allophane (Lowe *et al*., 1996; Lowe & Palmer, 2005; Takesako *et al*., 2010). For these reasons, it seems unlikely that Si concentrations are sufficiently low to limit halloysite formation. Rather, the presence of 2:1 type layer silicates, especially smectites, indicates that silica accumulation (resilication) has occurred in lower horizons of some of the soils because thermodynamically these clays require high Si activity for their formation (Dahlgren *et al*., 2004).

The profiles of two Mount Gambier/Schank soils are shown in Fig. 3a and 3b (see Lowe, 1992). The clay fraction of the soil from Brownes Lake (a Humic Vitrixerand) (Soil Survey Staff, 2014) near Mount Gambier (Fig. 3a) is dominated by kaolinite, illite, kaolinite-smectite, and/or illite-smectite in the upper horizons, and by allophane in the mid-lower

This is a 'pre-published' version of a paper accepted for publication in Clay Minerals.
This version may be changed during the production process.
The DOI, which may be used for citation purposes, but which will not be active until the version of record is published, is 10.1180/claymin.2016.051.3.14

horizons below 80 cm together with ferrihydrite (Lowe & Palmer, 2005). The allophane, comprising 11% of the whole soil (fine earth fraction) in the Bsm horizon at 80–82 cm, has an Al:Si ratio of 1.3, and hence is Si-rich. The clay fraction of the soil at Laslett Road (a Thaptic Haploxerand) near Mount Schank (Fig. 3b) contains little, if any, crystalline minerals. The clay-size material is dominated by allophane, making up 9, 13, and 9 % of the whole soil (fine earth fraction) in its uppermost three horizons to a depth of 70 cm, and contains substantial amounts of ferrihydrite (Lowe & Palmer, 2005). The Al:Si ratios of the allophane range from 1.7 in the uppermost Ap horizon, through 1.6 in the AB horizon, to 1.3 in the Bw horizon at 40–70 cm, indicating an abundance of Si-rich allophane, especially at depth. Hamblin & Greenland (1972) and Henmi & Wada (1976) have shown that allophane and small amounts of imogolite but not halloysite are present in the clay fractions of the Mount Schank soil. In Fig. 3c and d, the soils at Brownes Lake and Laslett Road, each ~5000 years old, are compared with profiles of two soils (Horotiu and Te Kowhai soils), each ~18,000 years old, in North Island, New Zealand. Formed on incrementally-accumulated volcanic ash overlying volcanogenic alluvium, the Horotiu soil (a Typic Hapludand) occurs in slightly elevated levees or channel bar landforms, manifest as low ridges or mounds. The Te Kowhai soil (a Typic Humaquept) is formed on fine volcanogenic alluvium in adjacent depressions or swales (Lowe, 2010). Being free-draining, and releasing Si on leaching (desilication), the Horotiu soil is rich in allophane, whereas the poorly-drained Te Kowhai soil accumulates Si in the soil solution, favouring halloysite formation (resilication) (Singleton *et al*., 1989; Lowe & Percival, 1993).

(Insert Fig. 3 about here)

It is notable therefore that halloysite is not present in the South Australian ash-derived soils that apparently developed under geological and climatic conditions similar to those conducive to halloysite formation in North Island, New Zealand, on rhyolitic to andesitic tephra, or in drier parts of Hawaii, on basaltic tephra. The result may indicate that under the xeric moisture regime at Mounts Gambier and Schank, winter rain is an especially effective leaching agent because potential evapotranspiration is at a minimum (Soil Survey Staff, 2014). These conditions are apparently conducive to the formation of Al-rich allophane in upper horizons, but the limited leaching over the non-winter months seems to favour formation of Si-rich allophane (and phyllosilicate clays) instead of halloysite.

Nevertheless, halloysite can form on ash and volcanogenic materials under xeric moisture regimes as Southard & Southard (1989) and Takahashi *et al*. (1993) have found in northern California (Churchman, 2015). Likewise, Jahn *et al*. (1987) have reported the occurrence of minor halloysite in a basaltic scoriaceous soil on Lanzarote (Canary Islands) under xeric conditions (although electron microscopy evidence was not presented). Hamblin & Greenland (1972) also found small amounts of 7 Å- and 10 Å-halloysite in soils formed under xeric moisture regimes from scoria at basaltic complexes at Tower Hill, Red Rock, and Mount Porndon in southwest Victoria, Australia, ~150–250 km to the east of Mounts Gambier and Schank. However, the parent materials of these three Victoria soils lack the highly calcareous component evident in the soils at Mounts Gambier and Schank. It would therefore appear that some factor(s) are inhibiting or preventing halloysite from forming at Mounts Gambier and Schank.

Table 1 compares the mineralogy of soils, formed from volcanic materials under a xeric moisture regime in South Australia (Mounts Gambier and Schank), with that of soils from

similar materials under a similar moisture regime in northern California. Like the volcanic ash soils in North Island, New Zealand, the northern California soils contain halloysite and allophane with an Al:Si ratio of ~2:1. By contrast, the South Australian soils contain kaolinite, kaolinite-smectite, illitic phases, smectite, and the allophane here has Al:Si ratios that are closer to 1:1 than 2:1 on average (these ratios generally diminish with increasing depth). Note, however, that the South Australian soils, with no halloysite, have high pHs (to 8.7) whereas those from northern California have pHs of 5.3−6.9 (Table 1).

(Insert Table 1 about here)

The high pH of the South Australian soils, is related to calcareous materials underlying both volcanic complexes. The pyroclastic deposits and soils may contain as much as 60% of exotic, non-volcanic materials, including xenolithic limestone fragments as noted above (Lowe *et al*., 1996; Lowe & Palmer, 2005; Churchman & Lowe, 2014).

We thus propose that pH plays a key role in the formation of halloysite, especially in the interlayer uptake of H_2O. The proposal is based on the difference in charge characteristics between the silica tetrahedral sheet and the alumina octahedral sheet. Zeta potential projections for halloysite (Abdullayev & Lvov, 2013, 2015) (Fig. 4) show that the two structural sheets have a different pattern of pH-dependent charge. The octahedral sheet is positively charged at all pHs below ~8, whereas the tetrahedral sheet is negatively charged at all pHs above ~2. Zeta potential measurements on tubular halloysite (Vergaro *et al.*, 2010) show that the mineral follows the pattern for the silica tetrahedral sheet which makes up the outer surface of tubes. In other words, the zeta potential plots for halloysite closely correspond with those for the silica sheet. In line with this observation, Pasbakhsh *et al*. (2013) reported that the zeta potentials of six tubular (non-spherical) halloysites from world-

This is a 'pre-published' version of a paper accepted for publication in Clay Minerals.
This version may be changed during the production process.
The DOI, which may be used for citation purposes, but which will not be active until the version of record is published, is 10.1180/claymin.2016.051.3.14

wide sources were always negative above pH 1.5. Atomic force microscopy measurements of adjacent crystal faces of a kaolinite similarly show that the silica tetrahedral face is negatively charged at pH > 4, whereas the alumina octahedral face is positively charged at pH < 6, and negatively charged at pH >8 (Gupta & Miller, 2010).

Following Abdullayev & Lvov (2013, 2015) and Vergaro et al., (2010), we propose that the two sheets making up a layer of halloysite have opposite charges between pH ~2 and ~8. Consequently, the alumina sheet would attract the oxygen 'end', and the silica sheet the hydrogen 'end', of H_2O molecules. This process provides a driving force for the uptake and retention of interlayer H_2O by halloysite. Although kaolinite has the same sheet structure as halloysite to provide the same driving force (Gupta & Miller, 2010), H_2O molecules are not retained in the interlayer space of kaolinite owing to the lack, or erratic supply, of water during its formation.

(Insert Fig. 4 about here)

This hypothesis is consistent with observations that halloysites tend to occur in acidic environments. As noted above, halloysite often forms highly concentrated deposits when acidified groundwater comes into contact with sediments, including calcareous sediments (Keeling, 2015). Reports on halloysite occurrences rarely provide pH data of the groundwater, or the alteration products. Table 2 lists the pH of several soils and weathering profiles in which halloysite occurs. In their review of volcanic soils, Dahlgren *et al*. (2004, p. 142) associated a pH range of 5–6 with the occurrence of halloysite, and a pH range of 6–7 with that of Si-rich allophane, in general accord with clay mineralogy and soil reaction data (Table 1) for the volcanic ash-derived soils at Mounts Gambier and Schank in South Australia.

This is a 'pre-published' version of a paper accepted for publication in Clay Minerals.
This version may be changed during the production process.
The DOI, which may be used for citation purposes, but which will not be active until the version of record is published, is 10.1180/claymin.2016.051.3.14

(insert Table 2 about here)

Nearly all the soil samples (generally different horizons) containing halloysite have an acidic pH (Table 2). Interestingly, the Fox clay halloysite deposit (Utah) was derived from a calcareous substrate, but had been altered by thermal waters with a slightly acidic pH (Ames & Sand, 1957). In apparent contradiction, Silber *et al*. (1994) reported that small amounts of halloysite formed from weathered tuffs in Israel had an exceptionally high pH. The evidence, however, is equivocal because neither the particle morphology nor chemical reactivity of the sample was assessed.

Churchman & Lowe (2014) and Churchman (2015) have proposed an alternative mechanism to explain why halloysite formation hardly occurs under alkaline conditions. They argued that after its formation but prior to drying, halloysite contains ferrous ions in its layer. The replacement of Al^{3+} by Fe^{2+} in the octahedral sheet of halloysite raises the layer charge and cation exchange capacity (CEC). Ferrous ions are favoured over ferric ions under wet conditions but become unstable in relation to solid phases such as siderite ($FeCO_3$) in a CO_2-rich system (Sposito, 1994), and ferrihydrite ($Fe_5HO_8.4H_2O$) in a CO_2-poor system, as pH rises (Sposito, 2008). Ferrous ions, therefore, are rarely found in solutions of pH ≥ 6. The absence of halloysite in the ash-derived soils near Mount Gambier and Mount Schank may be linked to the requirement for ferrous ions during the formation of halloysite.

The suggested involvement of ferrous ions in halloysite formation is consistent with the detection of ferrous ions (≤ 10% of total Fe) in the Mössbauer spectra of 3 halloysites from New Zealand that have apparently not been dried (J.D. Cashion, unpublished). This suggestion, however, is inconsistent with the absence of exchangeable cations in halloysite as indicated by quasi-elastic neutron scattering (Bordallo *et al*., 2008). Mössbauer

This is a 'pre-published' version of a paper accepted for publication in Clay Minerals.
This version may be changed during the production process.
The DOI, which may be used for citation purposes, but which will not be active until the version of record is published, is 10.1180/claymin.2016.051.3.14

spectroscopy has shown that kaolinites may also contain considerable proportions (up to 62%) of iron in the ferrous form (Murad & Cashion, 2004). Furthermore, halloysites containing minimal iron, such as the 'Patch' halloysite with only 0.11% total Fe (as Fe_2O_3) (Norrish, 1995), would probably not make the layer charge sufficiently negative (Norrish, 1995, measured a CEC of 12 cmol kg^{-1}) to attract cation-coordinated H_2O to the interlayer space, even if all the incorporated iron occurred in the ferrous state. Conversely, a difference in polarity between opposing sheets, as proposed above, would not raise either layer charge or CEC, and hence would not require exchangeable cations to balance an excess of negative charge.

Being variable in chemistry, morphology, and charge characteristics, different halloysites may employ a range of mechanisms for adsorbing and retaining interlayer H_2O., including the opposing polarities of adjacent sheets, substitution of Al^{3+} for Si^{4+} in tetrahedral positions, Fe^{2+} for Al^{3+} in the octahedral sheet, and the non-stoichiometric substitution of Fe^{3+} for Al^{3+} (e.g., Soma *et al.*, 1992).

CRYSTAL STRUCTURE

The X-ray diffraction (XRD) patterns of many halloysites lack (hkl) peaks, indicating that the structure lacks 3-dimensional order. Unless samples contain sufficient interlayer H_2O to give a basal spacing near 10 Å, the XRD patterns may be similar to those for disordered kaolinite. Halloysites are often analysed after sufficient drying to remove the 10 Å reflection. Initially, Brindley & Robinson (1946) proposed that halloysites are the end-members of a series of

This is a 'pre-published' version of a paper accepted for publication in Clay Minerals.
This version may be changed during the production process.
The DOI, which may be used for citation purposes, but which will not be active until the version of record is published, is 10.1180/claymin.2016.051.3.14

minerals, ranging from highly crystalline kaolinite, at one end, to highly disordered halloysite, at the other (Churchman & Carr, 1975). The information about tubular halloysite that accumulated by the early 1950s strongly suggested that the apparent lack of 3-dimenisonal order was related to layer curvature similar to that observed in chrysotile (Whittaker, 1954; Waser, 1955).

However, particles of halloysite are not necessarily curved. Although platy halloysites would not be expected to show the distorting effects from curvature, their X-ray diffraction patterns generally do not show that they are more ordered than those given by the tubular and other curved forms (cf. Fig. 5 in Joussein *et al*., 2005). The 3-dimensional order indicated by electron diffraction analysis (Honjo *et al*., 1954; Kulbicki, 1954; Chukrov & Zvyagin, 1966), may be related to halloysite having a 2-layer structure (Honjo *et al*., 1954; Chukhrov & Zvyagin, 1966; Kohyama *et al.*, 1978; Guggenheim, 2015). Prismatic forms of halloysite are possibly more ordered than other morphological forms of the mineral. On the basis of electron diffraction analysis, Chukhrov & Zvyagin (1966) have suggested that the prismatic form of (dehydrated) halloysite has the most ordered structure in that it has 2-layer regularity with ordered layer displacements producing a structural type distinct from that of kaolinite.

Using high resolution transmission electron microscopy (TEM), Kogure *et al*. (2011, 2013) found that a prismatic dehydrated halloysite showed 2-layer regularity over a small range of layers, but this feature is not necessarily related to layer stacking. Layer stacking shows single layers with random displacements. As predicted by Chukhrov & Zvyagin (1966), the displacement (by -a/3-b/3) is parallel to *[110]* but occurs in different directions within a crystal (Guggenheim, 2015). Kogure *et al*. (2013) also found reflections indicating some 3-

dimensional character that are not normally observed in the XRD patterns of halloysite. In particular, there are two sharp peaks with d-values of 4.28 and 4.03 Å, superimposed on the *(02,11)* band for halloysite. These two peaks are not observed for kaolinite. Following Chukhrov & Zvyagin (1966), the peaks are indexed as *(021)* and *(-112)* for a 2-layer cell, but cannot be ascribed to dickite which gives much stronger reflections nearby for different spacings (Kogure *et al*., 2013).

Working on complexes of halloysites with a range of amides, Churchman & Theng (1984) observed a number of peaks in the XRD patterns of some complexes in addition to those normally seen for halloysites. These previously unpublished observations are presented below, and the phenomenon is further explored by intercalating other organic compounds (pyridine, dimethyl sulphoxide), and removing the intercalants by washing and heating the complexes.

A number of peaks appear that are not present in the XRD patterns of hydrated (10 Å-) halloysite. Fig. 5 shows the XRD patterns of complexes of Opotiki halloysite with a range of amides. Peaks with values between 4.4 and 3.33 Å are visible, occurring between the peak values for the *(02,11)* and the *(003)* bands for hydrated halloysite. Similar patterns were also obtained for complexes of this halloysite with dimethylformamide (DMFA), N-methylacetamide (NMAA), dimethylacetamide (DMAA) and propionamide (PA), but these are not shown.

(Insert Fig. 5 about here)

There are three peaks, denoted a, b, and c, that are absent from the pattern of hydrated halloysite: peak a has a value of 4.10 to 4.16 Å as the basal spacing of the complex varies

from 10.4 Å for formamide (FA) to 11.0 Å for acetamide (AA); peak b with a value ranging from 3.92 to 3.97 Å, as the basal spacing varies from 10.4 Å (FA) to 11.0 Å (AA), and peak c at 3.83 Å that only appears in the formamide (FA) complex (basal spacing = 10.4 Å), being obscured by *(003)* peaks for complexes with larger basal spacings. Peak a has a value of 4.23 Å for the DMAA complex (pattern not shown), peak b has a value of 4.07 Å for the PA complex (pattern not shown), but this peak is obscured in complexes that have basal spacings higher than 11.2 Å (for the PA complex).

There is also a peak with values varying from 5.2 Å (FA) to 6.2 Å (DMAA – pattern not shown). Because the basal spacings vary from 10.4 Å (FA) to 12.4 Å (the DMAA complex), this peak is attributable to *(002)* reflections that are absent from the pattern of hydrated halloysite. In addition, new peaks occur at 2.69 Å for the N-methylformamide (NMFA) complex (10.4 Å basal spacing), which increases to 2.93 Å for the dimethyl formamide (DMFA) complex (12.2 Å basal spacing) – pattern not shown, and also at 2.26 Å for the acetamide (AA) complex (11.0 Å basal spacing), increasing to 2.34 Å for the dimethylformamide (DMFA) complex (12.4 Å spacing) – pattern not shown. In comparing the new peaks that appear in the XRD pattern of various organic complexes with those shown by hydrated halloysite (Fig. 5(i)), the corresponding spacings vary with the basal spacing of the complexes. Thus, their indices include an 'l' component, reflecting the different d-spacings (or lengths of the repeat distances along the 'c' axis).

Fig. 6 shows the relevant parts of the XRD patterns for dimethyl sulphoxide (DMSO) complexes of Opotiki halloysite, a low-crystalline kaolinite (KGa-2), a high-crystalline kaolinite (KGa-1), and a dickite (API, H-14). The complexes formed had identical basal spacings of 11.2±0.1 Å, allowing the presence or absence of peaks to be compared at the

same spacings. Only halloysite yielded complete complexes with DMSO, whereas the other kaolin minerals give mixtures of the DMSO complex and the original (uncomplexed) materials.

(Insert Fig. 6 about here)

Peaks, corresponding to *(002)* and *(003)* reflections, appear at identical positions of 5.6±0.1 Å and 3.73±0.4 Å respectively for all DMSO complexes (Fig. 6, but not shown for dickite). In each case, there is also a peak at 4.4 Å for the *(020)* reflection, or *(02,11)* band in halloysite (Fig. 6). Of particular interest in Fig. 6 are the four peaks between the 4.4 Å peak and the *(003)* reflection at 3.7 Å that are common to all four kaolin minerals. Labelled a, b, c, and d, these peaks are at 4.32 ± 0.3, 4.20 ± 0.2, 4.13 ± 0.1, and 4.10 ± 0.3 Å, respectively. One peak at 3.85 ± 0.3 Å only appears in the dickite pattern. The halloysite pattern in Fig. 6 may show a shoulder on the adjacent 'd' peak, with a raised minimum between this and the *(003)* peak at ~ 3.89 Å. The patterns of DMSO complexes with other halloysites (patterns not shown) may show small peaks at or near this spacing (3.90 ± 0.2 Å). Such peaks occur for Te Puke, Hamilton soil, and Te Akatea halloysites, but not for Matauri Bay, Dunedin, and Kauri halloysites.

Some of the peaks for (hkl) reflections from halloysite complexes with DMSO and also with pyridine are retained after washing, and even after washing and heating. The results for the pyridine complexes with Matauri Bay halloysite are shown in Fig. 7, and summarised in Table 3, where the peak values obtained are compared with those given in the literature for (untreated) kaolinite and dickite. The washed complex has a strong peak at 4.05 Å that is not present in the pattern for hydrated halloysites (cf. Fig. 5). This peak remains even after

the washed complex (basal spacing = 10.0 Å) has been heated at 110°C to drive out interlayer H_2O, reducing the basal spacing to 7.3 Å.

(Insert Fig. 7 about here)

(Insert Table 3 about here)

The appearance of new peaks in several organic complexes of halloysites and their behaviours (Figs. 5, 6, & 7; and Table 3), imply that one or more of the following changes have occurred during complex formation: (1), X-ray scattering from organic molecules, held within the complexes, is greater than that from water; and (2), there is re-alignment of halloysite layers relative to one another as a result of the attractive interactions between the intercalated organic molecules and aluminosilicate layers.

The appearance of new peaks in the XRD pattern of halloysite-organic complexes has also been reported by Sanchez Camazano & Gonzalez Garcia (1966), Jacobs & Sterckx (1970), Anton & Rouxhet (1977), and Costanzo & Giese (1986). Their conclusions are cited in the following analyses of our results.

Relatively intense *(002)* X-ray peaks for halloysite complexes with organic molecules, such as DMSO (Fig. 6) contrast with the absence of *(002)* peaks from the pattern of hydrated halloysite (Brindley, 1961). Calculations by Churchman (1970) indicate that an exceptionally weak reflection at the *(002)* position (5 Å) arises from scattering of water molecules positioned halfway between the layers of halloysite. Intercalated organic molecules, such as amides and DMSO, presumably occupy the same position (Adams, 1978; Thompson & Cuff, 1985).

The intercalation of organic molecules, especially DMSO, by kaolin minerals could also bring about considerable horizontal displacement of individual aluminosilicate layers relative to one another, to produce layer stacking disorder (Sanchez Camazano & Gonzalez Garcia, 1966; Anton & Rouxhet, 1977; Thompson & Cuff, 1985). Indeed, rolling of some hexagonal kaolinite flakes into a tubular shape, following intercalation of DMSO, was observed by Sanchez Camazano & Gonzalez Garcia (1966). In the case of halloysite, by contrast, organic complex formation appears to enhance layer stacking order. For instance, the appearance of a well-defined *(002)* peak with a value of 5.0 A in the XRD pattern of the washed pyridine complex (Fig. 7), is indicative of layer re-ordering following complex formation that is retained on rehydration to 10 A-halloysite.

Interestingly, Anton & Rouxhet (1977) have observed the apparent unrolling of halloysite tubes with DMSO in electron micrographs. On the basis of visual similarities in the XRD patterns and IR spectra between DMSO complexes of kaolinite and those of halloysite, these authors have suggested that DMSO intercalation into halloysite and subsequent washing of the complex transform halloysite (particularly a non-tubular form) into kaolinite. Costanzo & Giese (1986) have observed similarly, indicating "a fundamental equivalence in the structure of the silicate layer in both minerals". The comparisons of patterns within Fig. 6 tend to confirm this conclusion if based on complexes with only DMSO.

The persistence of the 4.05 Å peak in the pattern of re-ordered halloysite, after removing the organic intercalate by washing and then heating (Fig. 7), is noteworthy. Kogure *et al*. (2013) have observed a peak with this value for a dehydrated prismatic halloysite, and indexed it as *(-112)* on a 2-layer cell. The possibility that this peak is related to dickite, however, is rejected because dickite produces a number of strong peaks that are absent

from the pattern of re-ordered halloysite. These peaks have values of 4.12 Å and 3.79 Å, and there is a weaker peak at 3.98 Å, whereas kaolinite has weak peaks with values of 4.13 and 3.86 Å (Table 3). There is a possibility that the 4.12 Å peak for dickite is present but because its position is nearly coincident with a peak from the re-ordered halloysite, it would augment the corresponding peak for the halloysite complex. Any dickite component, however, would not remain expanded after washing, and hence the spacing would not change after washing or heating.

The origin of the peak with a value of 4.05 Å in the washed and heated halloysite-pyridine complex remains to be clarified, but this peak cannot be identified with any peaks in kaolinite. Peaks with a value of 4.05±0.08 Å appeared in the XRD patterns of halloysite complexes with all organic compounds tested, including DMSO. Thus, the realignment of halloysite layers as a result of organic complex formation does not appear to lead to a kaolinite layer stacking.

MORPHOLOGY

Most halloysites contain substantial Fe, up to 12.8% by weight of Fe_2O_3 (Joussein *et al*., 2005). The review by Joussein *et al*. (2005) shows a plot relating Fe content to particle shape (platy, long tubular, short tubular, spheroidal). There is a wide range of Fe contents within each of these four morphological classes but the platy forms of halloysite tend to have a high Fe content (e.g., Tazaki, 1982), whereas long-tubular forms tend to contain very little iron (e.g., Norrish, 1995). Iron in halloysites occurs in two main forms, namely, as Fe^{3+} (or Fe^{2+}) substituting for Al^{3+} in the octahedral sheet, or incorporated in oxides, oxyhydroxides and hydroxides of Fe, known collectively as 'Fe(hydr)oxides'. Because these compounds are

commonly and intimately associated with halloysite particles, the apparent relationship between Fe content and particle morphology may not be reliably attributed to structural Fe (Bailey, 1990). Nonetheless, the average length and width of eight mainly tubular halloysites from New Zealand (after treatment with dithionite to remove Fe (hydr) oxides) tend to decrease as the Fe content of samples increases (Churchman & Theng, 1984). Even so, there is a need to separate the effect of structural Fe from that of associated iron hydr(oxides) on the shape and size of halloysite particles.

The likely effect of associated Fe (and Mn) (hydr)oxides on the size of halloysite particles is illustrated in Fig. 8 with respect to halloysite formed in saprolites in Hong Kong. Little, if any Fe or Mn is present in the material shown in Fig. 8a. In this sample, the infill veins comprise mostly Al and Si, and crystal growth is not restrained, giving rise to exceptionally long halloysite tubes. Where the contents of either Mn or Fe as hydr(oxides), are high (Figs. 8b and 8c, respectively), the tubes are much shorter (Fig. 8c). Figs. 8b and 8c show that platy kaolinite has also formed, probably as a result of drying, inducing oxidation and formation of the metal hydr(oxides). The occurrence of many different sites of nucleation (Fe and/or Mn hydr(oxides), kaolinite, halloysite), may have restrained crystal growth for each of these minerals, including halloysite tubes.

(Insert Fig. 8 about here)

Discussions on the size of tubular particles in relation to iron content (Tazaki, 1982; Bailey, 1990; Joussein *et al.*, 2005) have often emphasised the relative length of tubes. Fig. 9 shows transmission electron micrographs (TEMs) of some halloysite samples, illustrating the possible relationship between Fe content and particle size/shape. The Fe content refer to total values, including contributions from Fe (hydr)oxides and structural Fe. The dithionite-

extractable Fe, from associated Fe(hydr)oxides , is small (~0.2%) for the Te Puke material (Fig. 9a), and negligible for Matauri Bay halloysite (Fig. 9b). The majority of particles in Te Puke halloysite with the highest total Fe content (Fig. 9a) are non-tubular although there are some short, thin tubes present. The Jarrahdale sample also has a high Fe content (Fig. 9c) but most of the tubular particles are thin and short. Of the two halloysites with low Fe contents, the Matauri Bay material consists of thick tubes with variable lengths, and the 'Patch' halloysite (Fig. 9d) has tubular particles of similar width to that of the Jarrahdale material , but they are much longer than any seen in Figs. 6a-c. It would therefore appear that the relationship between Fe content and particle size in tubular halloysites is not straightforward and remains unresolved. In the Matauri Bay sample (Fig. 9b),a low Fe content enables the tubular particles to grow in both length and width whereas in the Patch halloysite (Fig. 9d) tubular particles are allowed to grow in length with little restraint but not in width. If the structural Fe content in tubular halloysites exceeds a certain limit, non-tubular shapes are favoured, as exemplified by the Te Puke sample (Fig. 9a).

(Insert Fig. 9 about here)

(Insert Table 4 about here)

Microprobe analyses (A.W. Fordham, K. Norrish and G.J. Churchman, unpublished) confirm that the Fe content of individual particles within a sample of halloysite can vary with morphology (Table 4). In this case, particles with a spheroidal morphology (relatively rare for the Te Akatea and Kauri samples), have mean Fe/Al ratios that are significantly higher statistically (according to the Student t test) than values for tubular particles from the same sample. The mean Fe/Al ratios are compared with Opotiki halloysite which is largely composed of spheroidal particles. The spheroidal particles in the Kauri and Te Akatea

halloysites have mean Fe/Al values that are significantly lower than those for Opotiki halloysite. By contrast, the Si/Al values (1.09 ± 0.02) are constant over the entire range of particle shapes.

Analyses of Fe content in particles of spheroidal or tubular halloysite (Table 4) cannot distinguish Fe within the structures of halloysite from Fe in associated (hydr)oxides. These data suggest that spheroidal particles in Opotiki halloysite either contain or are associated with, more Fe than the tubular particles in the Kauri and Te Akatea samples. Note also that other particles such as blocky halloysite particles and non-halloysite particles can occur in substantial amounts in these samples (Churchman & Theng, 1984).

There is no consensus about the influence of Fe content on spheroidal shapes for halloysite (Bailey, 1990; Joussein *et al*., 2005; Churchman, 2015; Cravero & Churchman, 2016), even if some of the particles in the Te Puke, Kauri, and Te Akatea halloysites are spheroidal, and have a high Fe content (Table 4). Even so, some spheroidal halloysites with a high surface area, exemplified by Opotiki halloysite (Churchman *et al*., 1995), may adsorb appreciably greater amounts of Fe hydr(oxides) than their tubular counterparts. The origin of spheroidal halloysite awaits clarification (see also Cravero & Churchman, 2016).

X-ray photoelectron spectroscopy (XPS) further indicates that separate layers within a single halloysite particle may have different Fe contents (Soma *et al*., 1992). Describing the layers as 'onion skins', these workers have proposed that the chemical composition of successive 'skins' is inhomogeneous. In a particular environment, the outer layer reflects the solution composition of that environment which would be different from that for the layers below.

CONCLUSIONS

1. The formation of halloysite requires the constant presence of water. Where the supply of water is intermittent, or seasonal drying occurs, kaolinite tends to form, sometimes in alternation with halloysite. Thus halloysite tends to occur in the lower, wetter parts of weathering profiles.

2. Halloysite tends to form under acid pH conditions because the layer charge is pH-dependent. The octahedral sheet of the halloysite layer is positively charged at all values of pH below ~8, whereas the tetrahedral sheet is negatively charged at all pH values above ~2. As a result, the two sheets comprising a layer attract different polar ends of H_2O molecules, providing a driving force for the uptake and retention of H_2O in the interlayer space.

3. Layer re-alignment occurs, giving rise to new peaks for [hkl] reflections in the XRD pattern, when halloysite forms interlayer complexes with polar organic molecules. This process, however, does not lead to a kaolinite layer stacking, suggesting that halloysites are structurally different from kaolinites.

4. Organic complexes of halloysites show a tendency towards a 2-layer stacking order.

5. (Hydr)oxides of Fe and Mn are often closely associated with halloysites. These compounds are not part of the structure, but can affect the size of halloysite particles by restraining crystal growth.

This is a 'pre-published' version of a paper accepted for publication in Clay Minerals.
This version may be changed during the production process.
The DOI, which may be used for citation purposes, but which will not be active until the version of record is published, is 10.1180/claymin.2016.051.3.14

6. Halloysites with approximately platy particles often contain high structural Fe, whereas a low Fe content appears to be associated with exceptionally long tubular particles. Differently shaped particles within a given sample of halloysite may have different Fe contents.

ACKNOWLEDGMENTS

We thank Arthur Fordham and Keith Norrish, formerly of CSIRO Division of Soils, for the microprobe analyses and John Cashion, of Monash University, for access to his data and useful discussions regarding Mössbauer spectral analyses. We are grateful to Steve Guggenheim and two other reviewers and also Steve Hillier (as editor) for helpful comments on an earlier version of the manuscript.

REFERENCES

Abdullayev E. & Lvov Y. (2013) Halloysite clay nanotubes as a ceramic “skeleton” for functional biopolymer composites with sustained drug release. *Journal of Materials Chemistry* B, **1,** 2894-2903.

Abdullayev E. & Lvov Y. (2015) Halloysite tubule nanoreactors in industrial and agricultural applications. Pp. 363-382 in: *Natural Mineral Nanotubes* (P. Pasbakhsh & G.J. Churchman, editors). Apple Academic Press, Oakville, Canada.

Adams J.M. (1978) Unifying features relating to the 3D structures of some intercalates of kaolinite. *Clays and Clay Minerals*, **26**, 291-295.

Alexander L.T.; Faust G.T. Hendricks S.B., Insley H. & McMurdie H.F. (1943) Relationship of the clay minerals halloysite and endellite. *American Mineralogist*, **28**, 1-18.

Allison G.B. & Hughes M.W. (1978) The use of environmental chloride and tritium to estimate total recharge to an unconfined aquifer. *Australian Journal of Soil Research*, **16**, 181-195.

Ames l.L. & Sand L.B. (1957) Halloysite formed in a calcareous hot spring environment. *Clays and Clay Minerals*, **6**, 378-385.

Anton O. & Rouxhet P.G. (1977) Note on the intercalation of kaolinite and halloysite by dimethyl-sulfoxide. *Clays and Clay Minerals*, **25**, 259-263.

Bailey S.W. (1990) Halloysite: a critical assessment. Pp. 89-98 in: *Proceedings of the 9th International Clay Conference 1989* (V.C. Farmer & Y. Tardy, editors). Sciences Géologiques, Mémoire 86, Strasbourg, France.

Barbetti M. & Sheard M.J. (1981) Palaeomagnetic measurements from Mounts Gambier and Schank, South Australia. *Geological Society of Australia Journal*, **28**, 385-394.

Berthier P. (1826) Analyse de l'halloysite. *Annales de Chimie et de Physique*, **32**, 332-335.

Bordallo H. N., Aldridge L. P., Churchman G. J., Gates W. P., Telling M. T. F., Kiefer K., Fouquet P., Seydel T. & Kimber, S. A. J. (2008) Quasi-elastic neutron scattering studies on clay interlayer-space highlighting the effect of the cation in confined water dynamics. *Journal of Physical Chemistry* C, **112**, 13982–13991.

Brathwaite R.L., Christie A.B., Faure K., Townsend M.G. & Terlesk S. (2012) Origin of the Matauri Bay halloysite deposit, Northland, New Zealand. *Mineralium Deposita*, **47**, 897-910.

Brathwaite R.L., Christie A.B., Faure K., Townsend M.G. & Terlesk S. (2014) Geology, mineralogy and geochemistry of the rhyolite-hosted Maungaparerua clay deposit, Northland. *New Zealand Journal of Geology and Geophysics*, **57**, 357-368.

Brindley G.W. (1961) Kaolin, serpentine and kindred minerals. Pp. 51-131 in: *The X-Ray Identification and Crystal Structures of Clay Minerals* (G. Brown, editor). Mineralogical Society, London, UK.

Brindley G.W. & Robinson K. (1946) Randomness in the structures of kaolinitic clay minerals. *Transactions of the Faraday Society*, **42B**, 198-205.

Calvert C.S., Buol S.W. & Weed S.B. (1980) Mineralogical transformations of a vertical rock-saprolite-soil sequence in the North Carolina Piedmont. *Soil Science Society of America Journal*, **44**, 1096-1112.

Christidis G.E. (2013) Assessment of industrial clays. Pp. 425-450 in *Handbook of Clay Science*. *Part B. Techniques and Applications,* 2nd. edition (F. Bergaya & G. Lagaly, editors). Elsevier, Amsterdam, The Netherlands.

Chukhrov F.V. & Zvyagin B.B. (1966) Halloysite, a crystallochemically and mineralogically distinct species. *Proceedings of the International Clay Conference 1*966 (L. Heller & A. Weiss, editors). Israel Program for Scientific Translation, Jerusalem, Israel.

Churchman G.J. (1970) Interlayer water in halloysite. Unpublished PhD thesis lodged in the Library, University of Otago, Dunedin, New Zealand.

Churchman G.J. (1990) Relevance of different intercalation tests for distinguishing halloysite from kaolinite in soils. *Clays and Clay Minerals*, **38**, 591-599.

Churchman G.J., Davy T.J., Aylmore L.A.G., Gilkes R.J. & Self P.G. (1995) Characteristics of fine pores in some halloysites. *Clay Minerals*, **30**, 89-98.

Churchman G.J. (2000) The alteration and formation of soil minerals by weathering. Pp. F3-F76 in: *Handbook of Soil Science* (M.E. Sumner, editor). CRC Press, Boca Raton, Florida, USA.

Churchman G.J. 2010. Is the geological concept of clay minerals appropriate for soil science? A literature-based and philosophical analysis. *Physics and Chemistry of the Earth*, **35**, 927-940.

Churchman G.J. & Gilkes R.J. (1989) Recognition of intermediates in the possible transformation of halloysite to kaolinite. *Clay Minerals*, **24**, 579-590.

Churchman G.J. (2015) The identification and nomenclature of halloysite (a historical perspective). Pp. 51-67 in: *Natural Mineral Nanotubes* (P. Pasbakhsh & G.J. Churchman, editors). Apple Academic Press, Oakville, Canada.

Churchman G.J. & Carr R.M. (1975) The definition and nomenclature of halloysites. *Clays and Clay Minerals,* **23**, 382-388.

Churchman G.J. & Lowe, D.J. 2012. Alteration, formation and occurrence of minerals in soils. Pp. 20.1-20.72 in: *Handbook of Soil Sciences. Properties and Processes,* 2nd edition (P.M. Huang, Y. Li & M.E. Sumner, editors). CRC Press, Boca Raton, Florida, USA.

Churchman G.J. & Lowe D.J. (2014) Clay minerals in South Australian Holocene basaltic volcanogenic soils and implications for halloysite genesis and structure. Pp. 3-6 in: *Proceedings of the 23rd Biennial Australian Clay Minerals Society Conference, University of Western Australia, Perth* (R. Gilkes, editor). Published at http://www.smectech.com.au/ACMS/ACMS_Conferences/ACMS23/Program/Abstracts/S1-02%20Churchman%20and%20Lowe.pdf

Churchman G.J. & Theng B.K.G. (1984) Interactions of halloysites with amides: mineralogical factors affecting complex formation. *Clay Minerals*, **19**, 161-175.

Churchman G.J., Whitton J.S., Claridge G.G.C. & Theng B.K.G. (1984) Intercalation method using formamide for differentiating halloysite from kaolinite. *Clays and Clay Minerals*, **32**, 241-248.

Churchman G.J., Pontifex I.R. & McClure S.G. (2010) Factors affecting the formation and characteristics of halloysites or kaolinites in granitic and tuffaceous saprolites in

Hong Kong. *Clays and Clay Minerals*, **58**, 220-237.

Clay Minerals Society (2015). Glossary of Clay Terms April 2015. **http://www.clays.org/GLOSSARY/Clay_Glossary.htm** (accessed 22 January 2016)

Costanzo P.M & Giese R.F. Jr (1986) Ordered halloysite: dimethylsulfoxide intercalate. *Clays and Clay Minerals*, **43**, 105-107.

Cravero F. & Churchman G.J. (2016) The origin of spheriodal halloysite: a review of the literature. *Clay Minerals* (this issue).

Dahlgren R.A., Saigusa M. & Ugolini F.C. (2004) The nature, properties and management of volcanic soils. *Advances in Agronomy*, **82**, 113-182.

Dupuis C. & Ertus, R. (1995) The karstic origin of the type halloysite in Belgium. Pp. 262–366 in: *Clays Controlling the Environment – Proceeding of the 10th International Clay Conference, Adelaide 1993* (G. J. Churchman, R. W. Fitzpatrick & R. A. Eggleton, editors). CSIRO Publishing, Melbourne, Australia.

Eswaran H. & Wong Chaw Bin (1978) A study of a deep weathering profile on granite in Peninsular Malaysia. Parts I, II, and III. *Soil Science Society of America Journal* **42**, 144-158.

Eswaran H. & Yeow Yew Hong (1976) The weathering of biotite in a profile on gneiss in Malaysia. *Geoderma*, **16,** 9-20.

Fieldes M. (1968) Clay mineralogy. Pp. 22-39 in: *Soils of New Zealand, Part 2*. New Zealand Soil Bureau Bulletin, **26(2)**.

Fieldes M. & Swindale, L.D. (1954) Chemical weathering of silicates in soil formation. *New Zealand Journal of Science and Technology,* **B36**, 140-154.

Fordham A.W. & Norrish K (1974) Direct measurement of the composition of soil components which retain added arsenate, *Australian Journal of Soil Research* **12**, 165–172.

Galán E (2006) Genesis of clay minerals. Pp. 1129–1162 in*: Handbook of Clay Science* (F. Bergaya, B.K. G. Theng & G. Lagaly, editors). Developments in Clay Science, **1**, Elsevier, Amsterdam, The Netherlands.

Gouramanis C., Wilkins S. & De Deckker P. (2010) 6000 years of environmental changes recorded in Blue Lake, South Australia, based on ostracod ecology and valve chemistry. *Palaeogeography, Palaeoclimatology, Palaeoecology*, **297**, 223–237.

Guggenheim S. (2015). Phyllosilicates used as nanotube substrates in engineered materials: structures, chemistries, and textures. Pp. 4-48 in: *Natural Mineral Nanotubes* (P. Pasbakhsh & G.J. Churchman, editors). Apple Academic Press, Oakville, Canada.

Gupta V. & Miller J.D. (2010) Surface force measurements at the basal planes of ordered kaolinite particles. *Journal of Colloid and Interface Science* **344**, 362-371.

Hamblin A.P. & Greenland D.J. (1972) Mineralogy of soils from the Holocene volcanic area of southern Australia. *Australian Journal of Soil Research*, **10**, 61-72.

Henmi T. & Wada K. (1976) Morphology and composition of allophane. *American Mineralogist*, **61**, 379-390.

Hofmann U., Endell K. & Wilm D. (1934) Röntgenographische und kolloidchemische Untersuchungen über Ton. *Angewandte Chemie*, **47**, 539-547.

Honjo G., Kitamura N. & Mihama K. (1954) A study of clay minerals by means of single crystal electron diffraction diagrams – the structure of tubular kaolin. *Clay Minerals Bulletin*, **2**, 133-141.

Jacobs H. & Sterckx M. (1970) Contribution à létude de l'intercalation du diméthylsulfoxyde dans le réseau de la kaolinite. Pp. 154-160 in: *Reunion Hispano-Belga de Minerales de la Arcilla* (J.M. Serratosa, editor). Consejo Sup. Invest. Cient., Madrid, Spain.

Jahn R., Zarei M. & Stahr K. (1987) Formation of clay minerals in soils developed from basic volcanic rocks under semiarid climatic conditions in Lanzarote, Spain. *Catena*, **14**, 359-368.

Janik L.J. & Keeling J.L. (1993) FT-IR partial least-squares analysis of tubular halloysite in kaolin samples from the Mount Hope kaolin deposit. *Clay Minerals*, **28**, 365-378.

Joussein E., Petit S., Churchman J., Theng B., Righi D. & Delvaux B. (2005) Halloysite clay minerals – a review. *Clay Minerals*, **40**, 383-426.

Joussein E., Petit S & Delvaux B. (2007) Behaviour of halloysite clay under formamide treatment. *Applied Clay Science*, **35,** 17–24

Keeling J.L. (2015) The mineralogy, geology and occurrences of halloysite. Pp. 95-115 in: *Natural Mineral Nanotubes* (P. Pasbakhsh & G.J. Churchman, editors). Apple Academic Press, Oakville, Canada.

Keeling J.L., Self, P.G. & Raven, M.D. (2010) Halloysite in Cenozoic sediments along the Eucla Basin margin. *MESA Journal,* **59**, 9–13.

Kogure T., Mori K., Kimura Y. & Takai Y. (2011) Unraveling the stacking structure in tubular halloysite using a new TEM with computer-assisted minimal-dose system. *American Mineralogist,* **96**, 1776–1780.

Kogure T., Mori K., Drits V.A. & Takai Y. (2013) Structure of prismatic halloysite. *American Mineralogist*, **98***,* 1008–1016.

Kohyama N., Fukushima K. & Fukami A. (1978) Observation of the hydrated form of tubular halloysite by an electron microscope equipped with an environmental cell. *Clays and Clay Minerals*, **26**, 25-40.

Kulbicki G. (1954) Diagrammes de diffraction électronique de microcristaux de kaolinite et d'halloysite et observations sur la structure de ces mineraux. *Comptes rendus de l'Académie des Sciences*, *Paris,* **238**, 2405-2407.

Lagaly G., Ogawa M. & Dékány, I. (2013) Clay mineral-organic interactions. Pp. 437-505 in: *Handbook of Clay Science. Part A. Fundamentals,* 2nd edition (F. Bergaya & G. Lagaly, editors). Elsevier, Amsterdam, The Netherlands.

Lowe D.J. (1986) Controls on the rates of weathering and clay mineral genesis in airfall tephras: a review and New Zealand case study. Pp. 265-330 in: *Rates of Chemical Weathering of Rocks and Minerals* (S.M. Colman & D.P. Dethier, editors). Academic Press, Orlando, Florida, USA.

Lowe D.J. (1992) Profile descriptions of Quaternary basaltic volcanogenic soils of the Mount Gambier area, southeast South Australia. *CSIRO Division of Soils Technical Report*, **9/1992**, 1- 26.

Lowe D.J. (1995) Teaching clays: from ashes to allophane. Pp. 19-23 in: *Clays Controlling the Environment – Proceedings of the 10th International Clay Conference, Adelaide 1993*. (G.J. Churchman, R.W. Fitzpatrick & R.A. Eggleton, editors). CSIRO Publishing, Melbourne, Australia.

Lowe D.J. (2010) Introduction to the landscapes and soils of the Hamilton Basin. Pp. 1.24-1.61 in: *Guidebook for Pre-conference North Island, New Zealand "Volcanoes to Oceans" Field Tour. 19th World Soils Congress, International Union of Soil Sciences, Brisbane* (D.J. Lowe, V.E. Neall, M. Hedley, M, B. Clothier & A. Mackay). Soil and Earth Sciences Occasional Publication, **3**, Massey University, Palmerston North, New Zealand.

Lowe D.J. & Percival H.J. (1993) Clay mineralogy of tephras and associated paleosols and soils, and hydrothermal deposits, North Island. *Guidebook for Field Tour F1 – New Zealand*. 10th International Clay Conference, Adelaide, Australia, **F1**, 1-110.

Lowe D.J. & Nelson C.S. (1994) Guide to the nature and methods of analysis of the clay fraction of tephras in the South Auckland region, New Zealand. *Department of Earth Sciences, University of Waikato Occasional Report (Revised),* **11**, 1-69.

Lowe D.J., & Palmer, D.J. (2005) Andisols of New Zealand and Australia. *Journal of Integrated Field Science*, **2,** 39-65.

Lowe D.J., Churchman G.J., Merry R.H., Fitzpatrick R.W., Sheard M.J. & Hudnall W.H. (1996) Holocene basaltic volcanogenic soils of the Mt Gambier area, South Australia, are unusual globally: what do they tell us? *Proceedings of the Australian Society of Soil Science and New Zealand Society of Soil Science National Soils Conference,* University of Melbourne*,* Melbourne, Australia, **2**, 153-154.

MacEwan D.M.C. (1947) The nomenclature of the halloysite minerals. *Mineralogical Magazine*, **28**, 36-44.

Mehmel M. (1935) Über die Structur von Halloysit und Metahalloysit. *Zeitschrift für Kristallographie,* **90**, 35-43.

Mizota C. & van Reeuwijk L.P. (1989) Clay mineralogy and chemistry of soils formed in volcanic material in diverse climatic regions. *International Soil Reference and Information Centre Monograph,* **2**, 1-185*.*

Moon V.G., Lowe D.J., Cunningham M.J., Wyatt J., Churchman G.J., de Lange W.P., Mörz T., Kreiter S., Kluger M.O. & Jorat M.E. (2015) Sensitive pyroclastic-derived halloysitic soils in northern New Zealand: interplay of microstructure, minerals, and geomechanics. Pp. 3-21 in: *Volcanic Rocks and Soils. Proceedings of the International Workshop on Volcanic Rocks and Soils, Lacco Ameno, Ischia Island, Italy* (T. Rotonda, M. Cecconi, F. Silvestri & P. Tommasi, editors). Taylor & Francis, London, UK.

Murad E. & Cashion J. (2004) *Mössbauer Spectroscopy of Environmental Materials and Their Industrial Utilization.* Kluwer, Dordrecht, The Netherlands.

Murray-Wallace C.N. (2011) Comment on: "New $^{40}Ar/^{39}Ar$ ages for selected young (<1 Ma) basalt flows of the Newer Volcanic Province, southeastern Australia" by E. Matchan & D. Phillips. *Quaternary Geochronology*, **6**, 598-599.

Newman R.H., Childs C.W. & Churchman G.J. (1994) Aluminium coordination and structural disorder in halloysite and kaolinite by ^{27}Al NMR spectroscopy. *Clay Minerals,* **29**, 305-312.

NZ Soil Bureau (1968) Soils of New Zealand, Part 2. *New Zealand Soil Bureau Bulletin* **26 (2).**

Norrish K. (1995) An unusual fibrous halloysite. Pp. 275–284 in: *Clays Controlling the Environment – Proceedings of the 10th International Clay Conference, Adelaide 1993* (G.J. Churchman, R.W Fitzpatrick & R.A. Eggleton, editors). CSIRO Publishing, Melbourne, Australia.

Papoulis D., Tsolis-Katagas P. & Katagas C. (2004) Progressive stages in the formation of kaolinite from halloysite in the weathering of plagioclase. *Clays and Clay Minerals*, **52**, 271-285.

Parfitt R.L. (1990) Soils formed in tephra in different climatic regimes. *Transactions of the 14th International Congress of Soil Science, Kyoto*, **7**, 134-139.

Parfitt R.L. & Wilson A.D. (1985) Estimation of allophane and halloysite in three sequences of volcanic soils, New Zealand. *Catena Supplement*, **7**, 1-8.

Parfitt R.L., Russell M. & Orbell G.E. (1983) Weathering sequence of soils from volcanic ash involving allophane and halloysite, New Zealand. *Geoderma,* **29**, 41-57.

Parfitt R.L., Saigusa M. & Cowie J.D. (1984) Allophane and halloysite formation in a volcanic ash bed under differing moisture conditions. *Soil Science*, **138**, 360-364.

Parfitt R.L., Childs C.W. & Eden D.N. (1988) Ferrihydrite and allophane in four Andepts from Hawaii and implications for their classification. *Geoderma*, **41**, 223-241.

Pasbakhsh P., Churchman G.J. & Keeling J.L. (2013). Characterisation of properties of various halloysites relevant to their use as nanotubes and microfibre fillers. *Applied Clay Science*, **74**, 47-57.

Pochet G., Van der Velde M, Vanclooster M. & Delvaux B. (2007) Hydric properties of high charge, halloysitic clay soils from the tropical South Pacific region. *Geoderma* **138**, 96–109.

Polyak V.J. & Güven N. (1996) Alunite, natroalunite and hydrated halloysite in Carlsbad Cavern and Lechuguilla cave, New Mexico. *Clays and Clay Minerals,* **44**, 843-850.

Rasmussen C., Matsuyama N., Dahlgren R.A., Southard R.J. & Brauer N. (2007) Soil genesis and mineral transformation across an environmental gradient on andesitic lahar. *Soil Science Society of America Journal,* **71**, 225-237.

Renac C. & Assassi F. (2009) Formation of non-expandable 7 Å halloysite during Eocene–Miocene continental weathering at Djebel Debbagh, Algeria: A geochemical and stable-isotope study. *Sedimentary Geology,* **217**, 140–153.

Robertson G.B., Prescott J.R. & Hutton J.T. (1996) Thermoluminescence dating of volcanic activity at Mount Gambier, South Australia. *Royal Society of South Australia Transactions*, **120**, 7-12.

Ross G.J., Kodama H., Wang C., Gray J.T. & Lafreniere L.B. (1983) Halloysite from a strongly weathered soil at Mont Jacques Cartier, Quebec. *Soil Science Society of America Journal,* **47**, 327-332.

Saigusa M., Shoji S. & Kato T. (1978) Origin and nature of halloysite in Ando soils from Towada tephra. *Geoderma*, **20**, 115-129.

Sanchez Comazano M. & Gonzalez Garcia S. (1966) Complejos interlaminares de caolinita y haloisita con liquidos polares. *Anales de Edafologia y Agrobiologia*, **24**, 495-520.

Sheard M.J. (1990) A guide to Quaternary volcanoes in the Lower South-east of South Australia. *Mines and Energy Review South Australia*, **157**, 40-50.

Sheard M.J., Lowe D.J. & Froggatt P.C. (1993) Mineralogy of pyroclastic and lava deposits of Holocene basaltic volcanoes of Mts Gambier and Schank, South Australia. *Abstracts, IAVCEI International Volcanological Congress, Canberra*, p. 98.

Silber A., Bar-Yosef B., Singer A. & Chen Y. (1994) Mineralogical and chemical composition of three tuffs from northern Israel. *Geoderma*, **63**, 123-144.

Singer A., Zarei M., Lange F.M. & Stahr K. (2004) Halloysite characteristics and formation in the northern Golan Heights. *Geoderma*, **123**, 279-295

Singleton P.L., McLeod M. & Percival H.J. (1989) Allophane and halloysite content and soil solution silicon in soils from rhyolitic volcanic material, New Zealand. *Australian Journal of Soil Research*, **27**, 67-77.

Smith B.W. & Prescott J.R. (1987) Thermoluminescence dating of volcanic activity at Mt Schank, South Australia. *Australian Journal of Earth Sciences*, **34**, 335-342.

Soil Survey Staff (2014) *Keys to Soil Taxonomy, 12th edition.* USDA Natural Resources Conservation Service, 1-362.

Soma M., Churchman G.J. & Theng B.K.G. (1992) X-ray photoelectron spectroscopic analysis of halloysites with different composition and particle morphology. *Clay Minerals,* **27**, 413-421.

Southard S.B. & Southard R.J. (1989) Mineralogy and classification of andic soils in north-eastern California. *Soil Science Society of America Journal,* **53**, 1784-1791

Sposito G. (1994) *The Surface Chemistry of Natural Particles*. Oxford University Press, New York, USA.

Sposito G. 2008. *The Chemistry of Soils*, 2nd edition. Oxford University Press, New York, USA.

Środoń J. (2013) Identification and quantitative analysis of clay minerals. Pp. 25-49 in: *Handbook of Clay Science. Part B. Techniques and Applications*, 2nd edition (F. Bergaya & G. Lagaly, editors). Elsevier, Amsterdam, The Netherlands.

Stevens K.F. & Vucetich C.G. (1985) Weathering of Upper Quaternary tephras in New Zealand 2. Clay minerals and their climatic interpretation. *Chemical Geology*, **53**, 237-247.

Takahashi T., Dahlgren R. A. & van Susteren P. (1993) Clay mineralogy and chemistry of soils formed in volcanic materials in the xeric moisture regime of northern California. *Geoderma*, **59**, 131-150.

Takahashi T., Dahlgren R.A., Theng B.K.G., Whitton J.S. & Soma, M. (2001) Potassium-selective, halloysite-rich soils formed in volcanic materials from northern California. *Soil Science Society of America Journal*, **65**, 516-526.

Takesako H., Lowe D.J., Churchman G.J. & Chittleborough D.J. (2010) Holocene volcanic soils in the Mt. Gambier region, South Australia. Pp. 47-50 in: *Proceedings of the 19th World Congress of Soil Science, International Union of Soil Sciences, Brisbane, Symposium 1.3.1* (R.J. Gilkes & N. Prakongkep, editors). Published at http://www.iuss.org (World Soil Congresses).

Tazaki K. (1979) Micromorphology of halloysites produced by weathering of plagioclase in volcanic ash. Pp. 415-422 in: *Proceedings of the 6th International Clay Conference 1978* (M.M. Mortland & V.C. Farmer, editors). Developments in Sedimentology, **27**, Elsevier, Amsterdam, The Netherlands.

Tazaki K. (1982) Analytical electron microscopic studies of halloysite formation processes: morphology and composition of halloysite. Pp. 573-584 in: *Proceedings of the 7th International Clay Conference* 1981 (H. Van Olphen & F. Veniale, editors). Developments in Sedimentology, **35**, Elsevier, Amsterdam, The Netherlands.

Tazaki K. (2005) Microbial formation of a halloysite-like mineral. *Clays and Clay Minerals*, **53**, 224-233.

Theng B.K.G., Churchman G.J., Whitton J.S. & Claridge G.G.C. (1984) Comparison of intercalation methods for differentiating halloysite from kaolinite. *Clays and Clay Minerals*, **32**, 249-258.

Thompson J.G. & Cuff C. (1985) Crystal structure of kaolinite-dimethylsulfoxide intercalate. *Clays and Clay Minerals*, **33**, 490-500.

Torn M.S., Trumbore S.E., Chadwick O.A., Vitousek P.M. & Hendricks D.M. (1997) Mineral control of soil organic carbon storage and turnover. *Nature*, **389**, 170-173.

Ugolini F.C. & Dahlgren R.A. (2002) Soil development in volcanic ash. *Global Environmental Research*, **6**, 69-81.

van Otterloo J., Cas R.A.F. & Sheard M.J. (2013) Eruption processes and deposit characteristics at the monogenetic Mt. Gambier Volcanic Complex, SE Australia: implications for alternating magmatic and phreatomagmatic activity. *Bulletin of Volcanology*, **75, 737** (pp. 1-21).

Vergaro V., Abdullayev E., Lvov Y.M., Zeitoun A., Cingolani R., Rinaldi R. & Leporatti S. (2010) Cytocompatibility and uptake of halloysite clay nanotubes. *Biomacromolecules*, **11**, 820–826.

Waser J. (1955) Fourier transforms and scattering intensities of tubular objects. *Acta Crystallographica*, **8**, 142-150.

Whittaker E.J.W. (1954) The diffraction of X-rays by a cylindrical lattice. *Acta Crystallographica*, **7**, 827-837.

Ziegler K., Hsieh J.C.C., Chadwick O.A., Kelly E.F., Hendricks D.M. & Savin S.M. (2003) Halloysite as a kinetically controlled end product of arid-zone basalt weathering. *Chemical Geology*, **202**, 461-478.

Figure captions

Fig. 1: (a) Lateritic profile on dolerite at Jarrahdale, Western Australia; and (b) halloysite (dark shade) and kaolinite (light shade) measured as fractions of the clay content by expansion with formamide in the profile shown in (a) (data from Churchman & Gilkes, 1989). The profile in (a) spans approximately 8-9 metres from the surface to the saprolite above the consolidated rock on which the lower person is standing.

Fig. 2: (a), White veins or infill in saprolite on granite; (b), white veins in volcanic tuff surrounded and intercepted by manganese oxide; (c), SEM of white veins in a showing halloysite with long tubes often parallel to one another and occurring in bunches; and (d) SEM of white veins in (b) showing large, platy kaolinite particles, stacked in “books”; all from Hong Kong (from Churchman *et al*., 2010).

Fig. 3. Profiles of soils on volcanic ash or unconsolidated volcanogenic materials: (a) a Humic Vitrixerand mainly on basaltic ash at Brownes Lake near Mount Gambier, South Australia (marks on auger at 10-cm intervals); (b) a Thaptic Haploxerand on basaltic ash over a buried soil on aeolian sand at Laslett Road near Mount Schank, South Australia (knife ~25 cm long); (c) a Typic Hapludand (Horotiu soil) on mainly rhyolitic ash over coarse volcanogenic alluvium at Hamilton, New Zealand (cutting tool ~30 cm long) (from Lowe, 2010); and (d) a Typic Humaquept (Te Kowhai soil) on fine volcanogenic (rhyolitic glass-rich) alluvium at Hamilton, New Zealand (from Lowe, 2010; photo by P.L. Singleton).

Fig. 4. Schematic diagram of variation of the surface (zeta) potentials of the alumina and silica sheets of halloysite with solution pH (adapted from Abdullayev & Lvov, 2013; 2015).

Fig. 5. XRD (Co Kα radiation) of a selected area of spacings of complexes of Opotiki spheroidal halloysite with different amides on ceramic tiles prepared as in Churchman & Theng (1984); letters indicate 'extra' peaks. Values for the *(003)* peaks are: (i) 3.30 ± 0.05 Å; (ii) 3.40 ± 0.05 Å; (iii) 3.60 ± 0.05 Å; 3.65 ± 0.05 Å. Fig. 6. XRD (Co Kα radiation) of a selected area of spacings of complexes with dimethylsulphoxide (DMSO) of Opotiki (Op) spheroidal halloysite, a kaolinite with low crystallinity (KGa-2), a kaolinite with high crystallinity (KGa-1), and dickite (API, H-14); letters indicate 'extra' peaks. The complexes were formed by soaking the clays in laboratory-grade DMSO for ~ 1 day for halloysite, and 27 days for the kaolinites and dickite. The complexes with KGa-2, KGa-1 and dickite were incompletely formed; that with the halloysite was completely formed. Values for the *(002)* peaks shown are 5.6 ± 0.1 Å and those for the *(003)* peaks are 3.75 ± 0.05 Å. Fig. 7. XRD (Co Kα radiation) traces of a selected area of spacings of complexes of Matauri Bay (MB) tubular halloysite with pyridine (halloysite reacted with laboratory grade pyridine in stoppered glass tubes for 11 months), after washing the complex 10 times with water, and after heating the washed complex at 110^{o}C for 24 h. The *(003)* peak for the pyridine complex has a value of 4.0 ± 0.1 Å, and for the washed complex, a value of 3.40 ± 0.05 Å; the *(002)* peak for the washed complex has a value of 5.0 ± 0.1 Å, and for the heated washed complex, a value of 3.65 ± 0.05 Å.

Fig. 8. Effect of Fe and/or Mn in the environment of formation on the length of the halloysite tubes formed in infill in saprolites on granite in Hong Kong: scanning electron micrographs at left; EDX analyses from the same areas of infill (from Churchman, 2010, and Churchman *et al*., 2010). Permission for re-use kindly given by the Civil Engineering and Development Department, Hong Kong, and by Elsevier, publisher of *Physics and Chemistry of the Earth.*

Fig. 9. Transmission electron micrographs showing shapes and sizes of some halloysite particles in relation to their content of iron: (a) Te Puke (New Zealand), mostly platy, 0.2% Fe_2O_3 as oxides; (b) Matauri Bay (New Zealand), thick tubes, no Fe oxide; (c) Jarrahdale (Australia), short tubes, oxides not determined; and (d) Patch (Australia), very long tubes, small but variable Fe oxide content.

Tables

Table 1. Comparison of soils formed from volcanic ash under similar soil moisture and temperature regimes in South Australia and northern California.

Table 2. Some occurrences of halloysite in relation to pH.

Table 3. Peak spacings > 3.7 Å from Fig. 7 for the complex of Matauri Bay halloysite (MBH) with pyridine, after it has been washed with water and after this product has been heated at 110^{o}C. They are compared with the spacings of peaks for (untreated) kaolinite and dickite. Peak spacings in bold indicate the strongest peaks.

Table 4. Contents of Fe in relation to Al and of Al in relation to Si in individual particles of different shapes in <2 μm fractions of halloysite clays that were re-dispersed in water using an ultrasonic probe and dried on to electron microscope grids. Microprobe analyses were carried out following Fordham & Norrish (1974).

Table 1. Comparison of soils formed from volcanic ash under similar soil moisture and temperature regimes in South Australia and northern California.

Region	**MAP (mm)**	**Moisture & temperature regimes**[1]	**pH**	**Clay mineralogy**
Mts Gambier/ Schank	700	Xeric, Mesic	6.5-8.7	Allophane (Al:Si 2:1–1:1), kaolinite, kaolinite-smectite, illite, illite-smectite, (some) smectite
Northern California[2]	1000	Xeric, Mesic	5.3-6.9	Halloysite, allophane (Al:Si 2:1), (often) gibbsite, kaolinite?

[1] Soil Survey Staff (2014); [2] Takahashi *et al*. (1993)

Table 2. Some occurrences of halloysite in relation to pH

Occurrence	**Genesis**	**pH (method)**		**Halloysite**	**Reference** (number
		(water)	M KCl (or?)	**identification**	by date order)
Soil on granite (Malaysia)	Weathering	4.2-4.9	3.75-4.10	XRD, TEM, SEM, DTA	4, 5
2 soils (New Zealand)	Weathering of ash	4.7-5.9	4.2-5.0	XRD, TEM	2
Strongly weathered soil (Canada)	W'd biotite, feldspar		4.2 ($CaCl_2$)	XRD/f'de*, TEM, SEM, DTA	7
Soil on gneiss (Malaysia)	Weathered biotite	5.2-5.8		XRD, TEM, SEM, DTA	3
Soil on tephra (Japan)	Weathering of tephra	5.3-6.7		XRD, NaOH dissolution	6
5 soils (California)	Weathering of ash	5.7-6.9		XRD/f'de, TEM	8
3 soils on tephra (Pacific Islands)	Weathering of tephra	5.8-7.3	5.0-6.8	XRD/f'de	11
Microbially synthetic halloysite	Microbial synthesis	6-7.4		XRD, IR, TEM	10
Fox clay deposit (Utah)	Calcareous hot springs	6-7.5		XRD, TEM	1
3 weathered tuffs (Israel)	Weathering of tuffs	7.9-9.3	6.6-7.8	IR, DTA	9

*w'd = weathered, f'de = formamide test; (1) Ames & Sand (1957); (2) NZ Soil Bureau (1968); (3) Eswaran & Yeow (1976); (4, 5) Eswaran & Wong, Parts I and 2 (1978); (6) Saigusa et al. (1978); (7) Ross et al. (1983); (8) Takahashi et al. (1993); (9) Silber et al. (1994); (10) Tazaki, (2005); (11) Pochet et al. (2007)

Table 3. Peak spacings > 3.7 Å from Fig. 7 for the complex of Matauri Bay halloysite (MBH) with pyridine, after it has been washed with water and after this product has been heated at 110^{o}C. They are compared with the spacings of peaks for (untreated) kaolinite and dickite. Peak spacings in bold indicate the strongest peaks.

Sample	**Peak Spacing (Å)** *(Index)*						
MBH-pyridine	**11.9**		4.30	**4.17**	**?** **obsc. by** ***(003)***		3.75
MBH-pyr. H_2O wash	**10.0**	**5.0**	**4.26**		**4.04**		
MBH-pyr. $H_20/110^{o}$	**7.3**		4.27		**4.05**		
Kaolinite	**7.2** *(001)*			**4.18** *(11-1)*	4.13 *(1-1-1)*	3.86 *(02-1)*	
Dickite	**7.2** *(002)*		4.26 *(021)*		**4.12** *(11-2)*	3.98 *(111)*	**3.79** *(022)*

obsc. obscured

Table 4. Contents of Fe in relation to Al and of Al in relation to Si in individual particles of different shapes in <2 μm fractions of halloysite clays that were re-dispersed in water using an ultrasonic probe and dried on to electron microscope grids. Microprobe analyses were carried out following Fordham & Norrish (1974).

Halloysite:	Occurrence		Spheroidal			Tubular			Fe_2O_3	
	Sph.	Tub.	Fe/Al	Si/Al	No.	Fe/Al	Si/Al	No.	Sph.	Tub.
	%		(mean value)			(mean value)			%	
Kauri	3	62	0.10	1.09	[22]	0.06	1.11	[35]	3.3	2.0
Te Akatea	3.5	86	0.15	1.10	[17]	0.09	1.07	[16]	5.1	2.7
Opotiki	87	-	0.19	1.09	[22]	-	-	-	6.1	-

Sph. = spheroidal and Tub. = tubular forms, data from Churchman & Theng (1984); No. = number of particles analysed.

Fig. 1

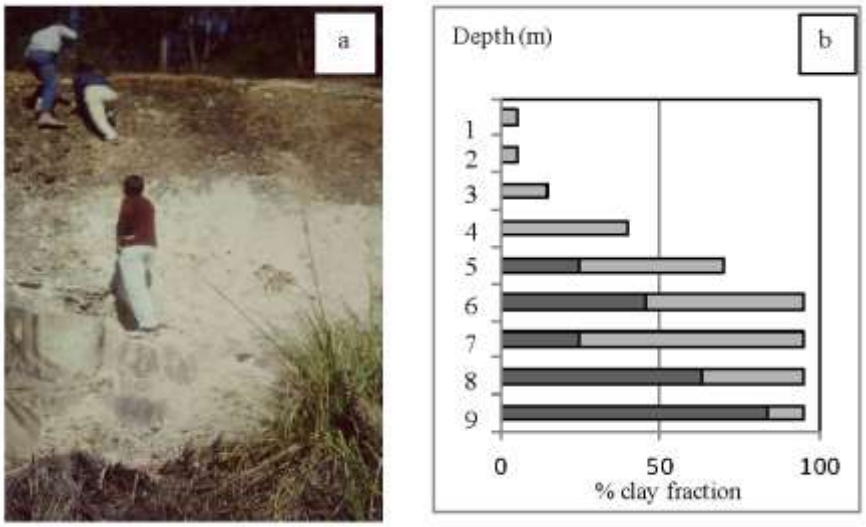

Fig. 2

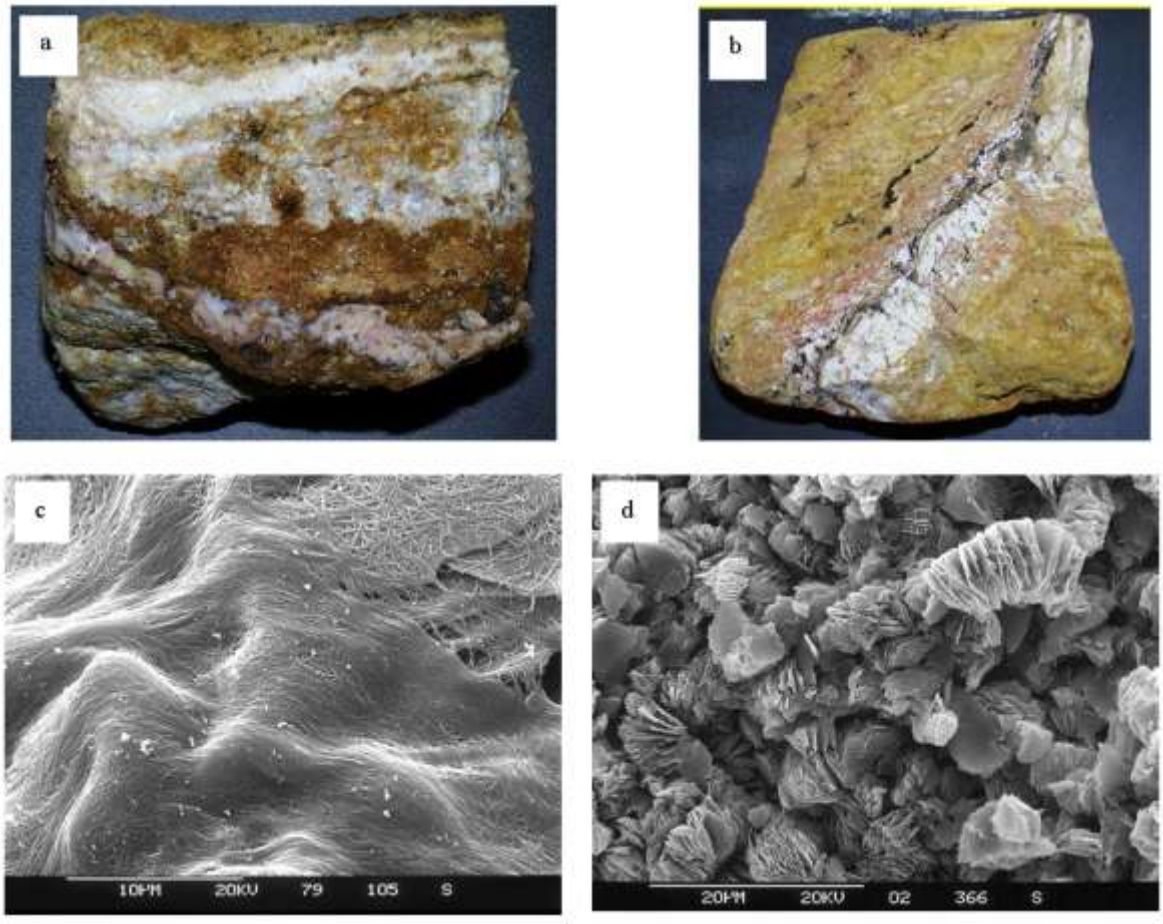

This is a 'pre-published' version of a paper accepted for publication in Clay Minerals.
This version may be changed during the production process.
The DOI, which may be used for citation purposes, but which will not be active until the version of record is published, is 10.1180/claymin.2016.051.3.14

Table 1. Comparison of soils formed from volcanic ash under similar soil moisture and temperature regimes in South Australia and northern California.

Region	**MAP (mm)**	**Moisture & temperature regimes**[1]	**pH**	**Clay mineralogy**
Mts Gambier/ Schank	700	Xeric, Mesic	6.5-8.7	Allophane (Al:Si 2:1–1:1), kaolinite, kaolinite-smectite, illite, illite-smectite, (some) smectite
Northern California[2]	1000	Xeric, Mesic	5.3-6.9	Halloysite, allophane (Al:Si 2:1), (often) gibbsite, kaolinite?

[1] Soil Survey Staff (2014); [2] Takahashi *et al*. (1993)

Table 2. Some occurrences of halloysite in relation to pH

Occurrence	**Genesis**	**pH (method)**		**Halloysite**	**Reference** (number
		(water)	M KCl (or?)	**identification**	by date order)
Soil on granite (Malaysia)	Weathering	4.2-4.9	3.75-4.10	XRD, TEM, SEM, DTA	4, 5
2 soils (New Zealand)	Weathering of ash	4.7-5.9	4.2-5.0	XRD, TEM	2
Strongly weathered soil (Canada)	W'd biotite, feldspar		4.2 ($CaCl_2$)	XRD/f'de*, TEM, SEM, DTA	7
Soil on gneiss (Malaysia)	Weathered biotite	5.2-5.8		XRD, TEM, SEM, DTA	3
Soil on tephra (Japan)	Weathering of tephra	5.3-6.7		XRD, NaOH dissolution	6
5 soils (California)	Weathering of ash	5.7-6.9		XRD/f'de, TEM	8
3 soils on tephra (Pacific Islands)	Weathering of tephra	5.8-7.3	5.0-6.8	XRD/f'de	11
Microbially synthetic halloysite	Microbial synthesis	6-7.4		XRD, IR, TEM	10
Fox clay deposit (Utah)	Calcareous hot springs	6-7.5		XRD, TEM	1
3 weathered tuffs (Israel)	Weathering of tuffs	7.9-9.3	6.6-7.8	IR, DTA	9

*w'd = weathered, f'de = formamide test; (1) Ames & Sand (1957); (2) NZ Soil Bureau (1968); (3) Eswaran & Yeow (1976); (4, 5) Eswaran & Wong, Parts I and 2 (1978); (6) Saigusa et al. (1978); (7) Ross et al. (1983); (8) Takahashi et al. (1993); (9) Silber et al. (1994); (10) Tazaki, (2005); (11) Pochet et al. (2007)

Table 3. Peak spacings > 3.7 Å from Fig. 7 for the complex of Matauri Bay halloysite (MBH) with pyridine, after it has been washed with water and after this product has been heated at 110^{o}C. They are compared with the spacings of peaks for (untreated) kaolinite and dickite. Peak spacings in bold indicate the strongest peaks.

Sample	**Peak Spacing (Å)** *(Index)*						
MBH-pyridine	**11.9**		4.30	**4.17**	**?** **obsc. by** ***(003)***		3.75
MBH-pyr. H_2O wash	**10.0**	**5.0**	**4.26**		**4.04**		
MBH-pyr. $H_20/110^{o}$	**7.3**		4.27		**4.05**		
Kaolinite	**7.2** *(001)*			**4.18** *(11-1)*	4.13 *(1-1-1)*	3.86 *(02-1)*	
Dickite	**7.2** *(002)*		4.26 *(021)*		**4.12** *(11-2)*	3.98 *(111)*	**3.79** *(022)*

obsc. obscured

Table 4. Contents of Fe in relation to Al and of Al in relation to Si in individual particles of different shapes in <2 μm fractions of halloysite clays that were re-dispersed in water using an ultrasonic probe and dried on to electron microscope grids. Microprobe analyses were carried out following Fordham & Norrish (1974).

Halloysite:	Occurrence		Spheroidal			Tubular			Fe_2O_3	
	Sph.	Tub.	Fe/Al	Si/Al	No.	Fe/Al	Si/Al	No.	Sph.	Tub.
	%		(mean value)			(mean value)			%	
Kauri	3	62	0.10	1.09	[22]	0.06	1.11	[35]	3.3	2.0
Te Akatea	3.5	86	0.15	1.10	[17]	0.09	1.07	[16]	5.1	2.7
Opotiki	87	-	0.19	1.09	[22]	-	-	-	6.1	-

Sph. = spheroidal and Tub. = tubular forms, data from Churchman & Theng (1984); No. = number of particles analysed.

Fig. 3

Fig. 4

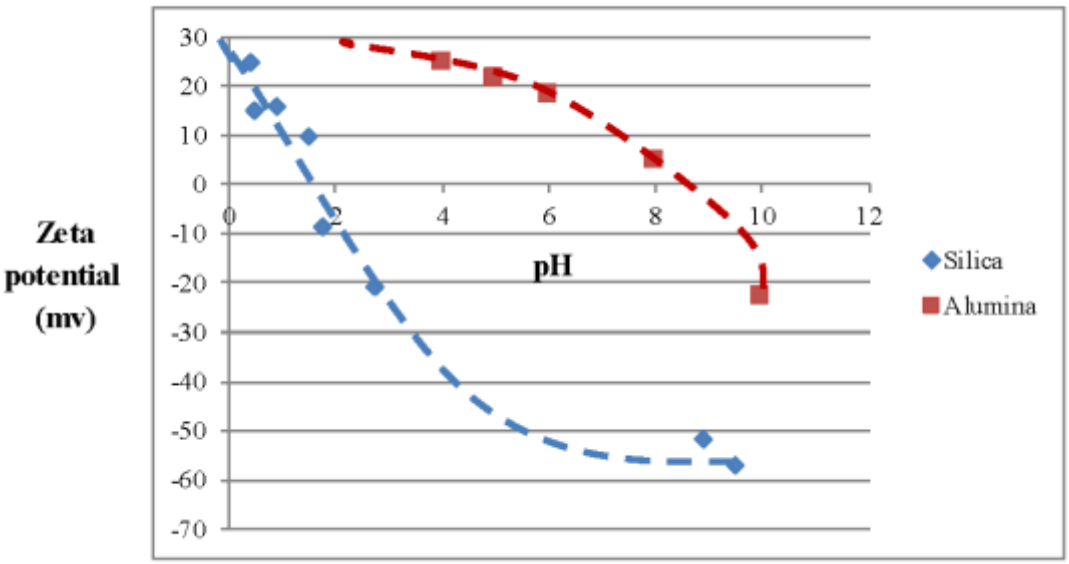

This is a 'pre-published' version of a paper accepted for publication in Clay Minerals.
This version may be changed during the production process.
The DOI, which may be used for citation purposes, but which will not be active until the version of record is published, is 10.1180/claymin.2016.051.3.14

Fig. 5

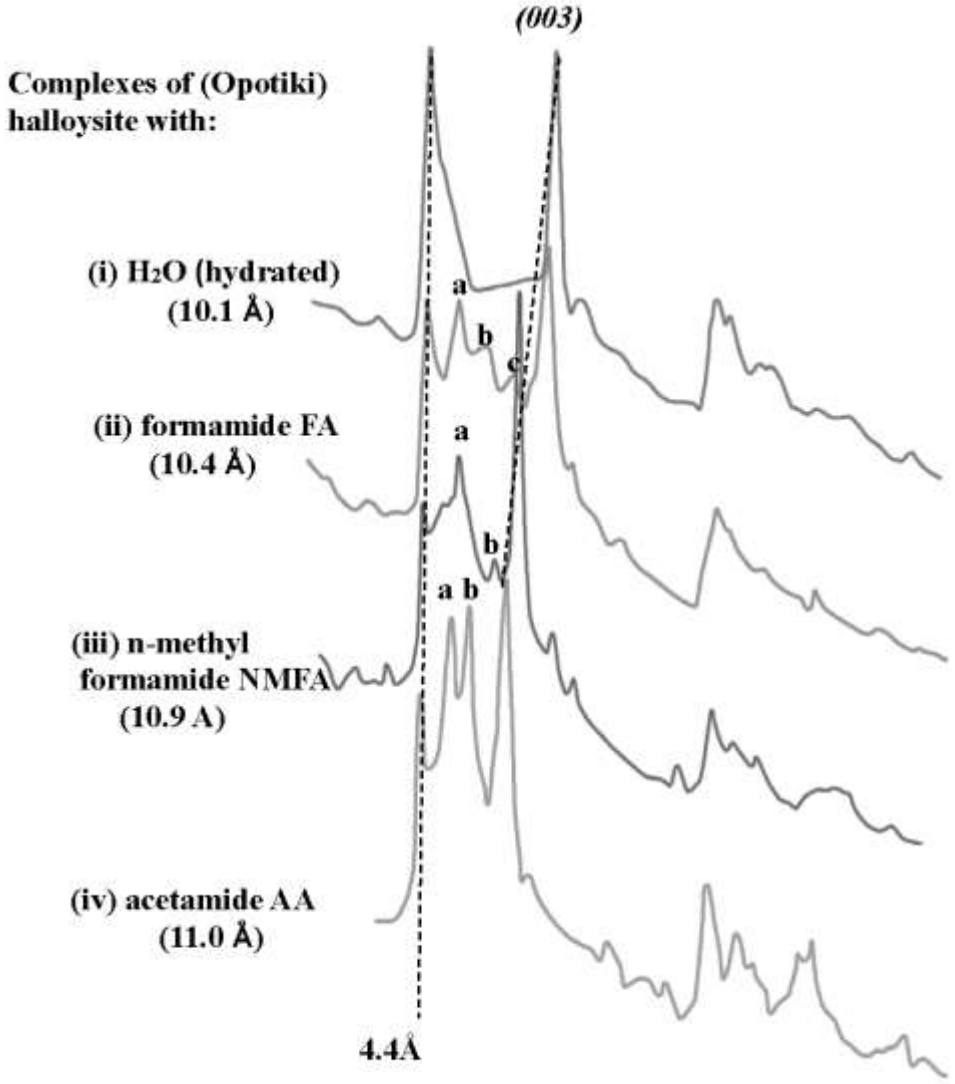

Fig. 6

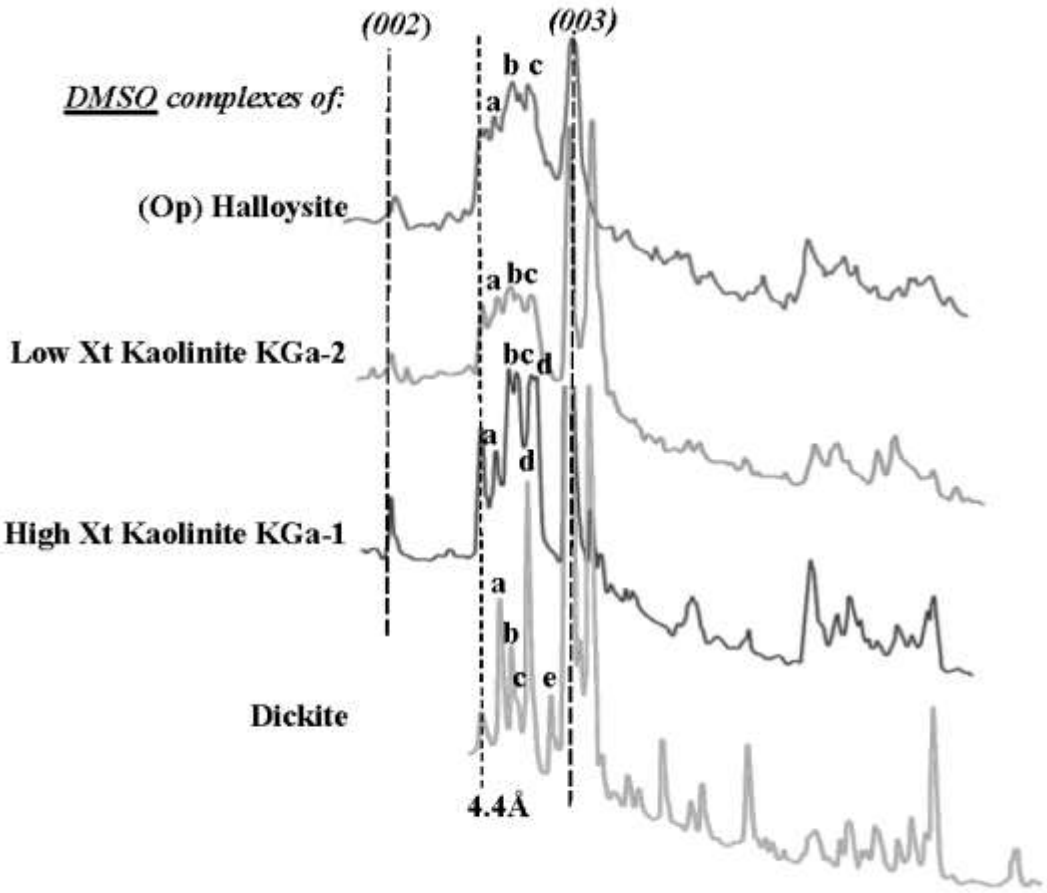

Fig. 7

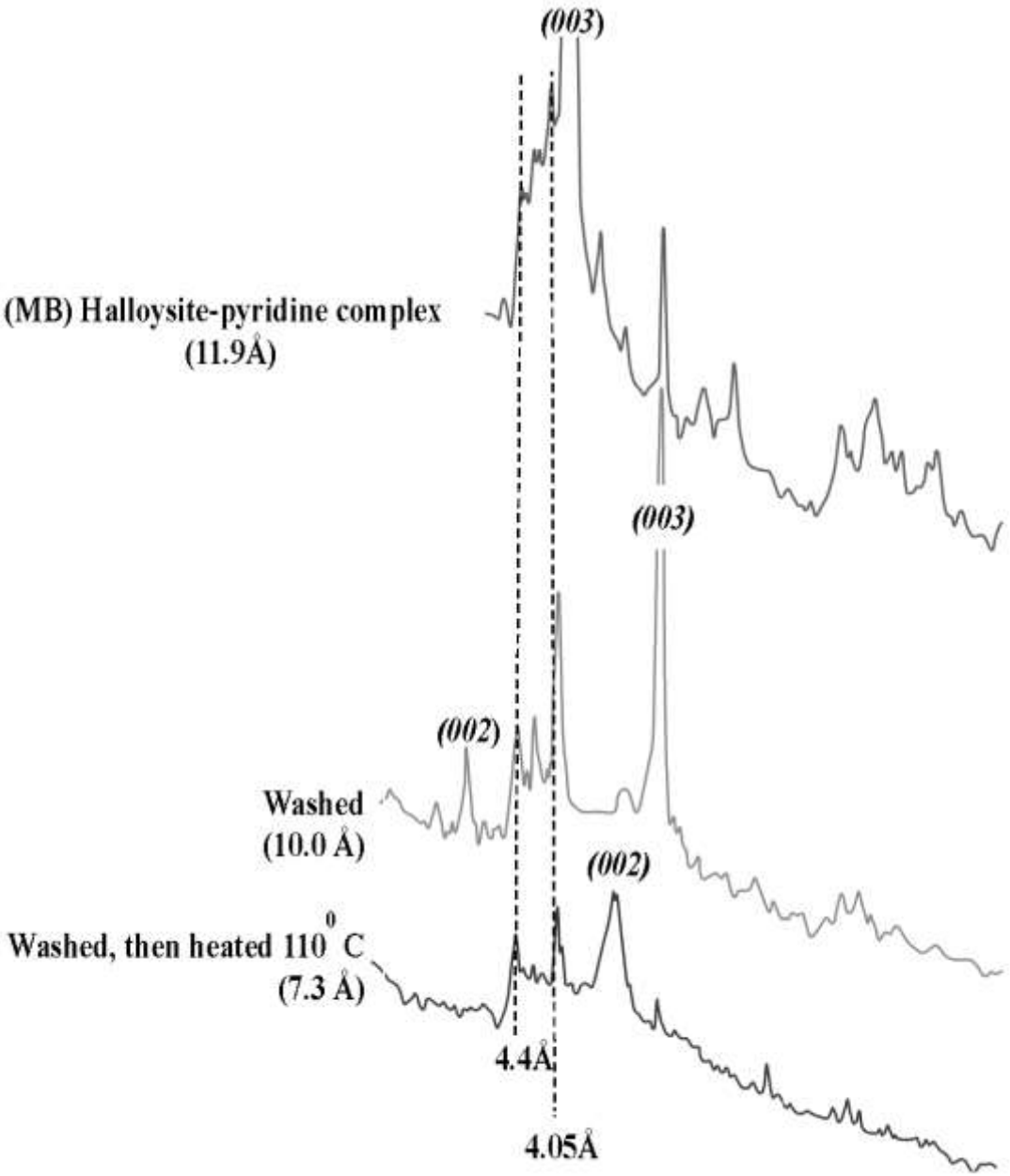

Fig. 8

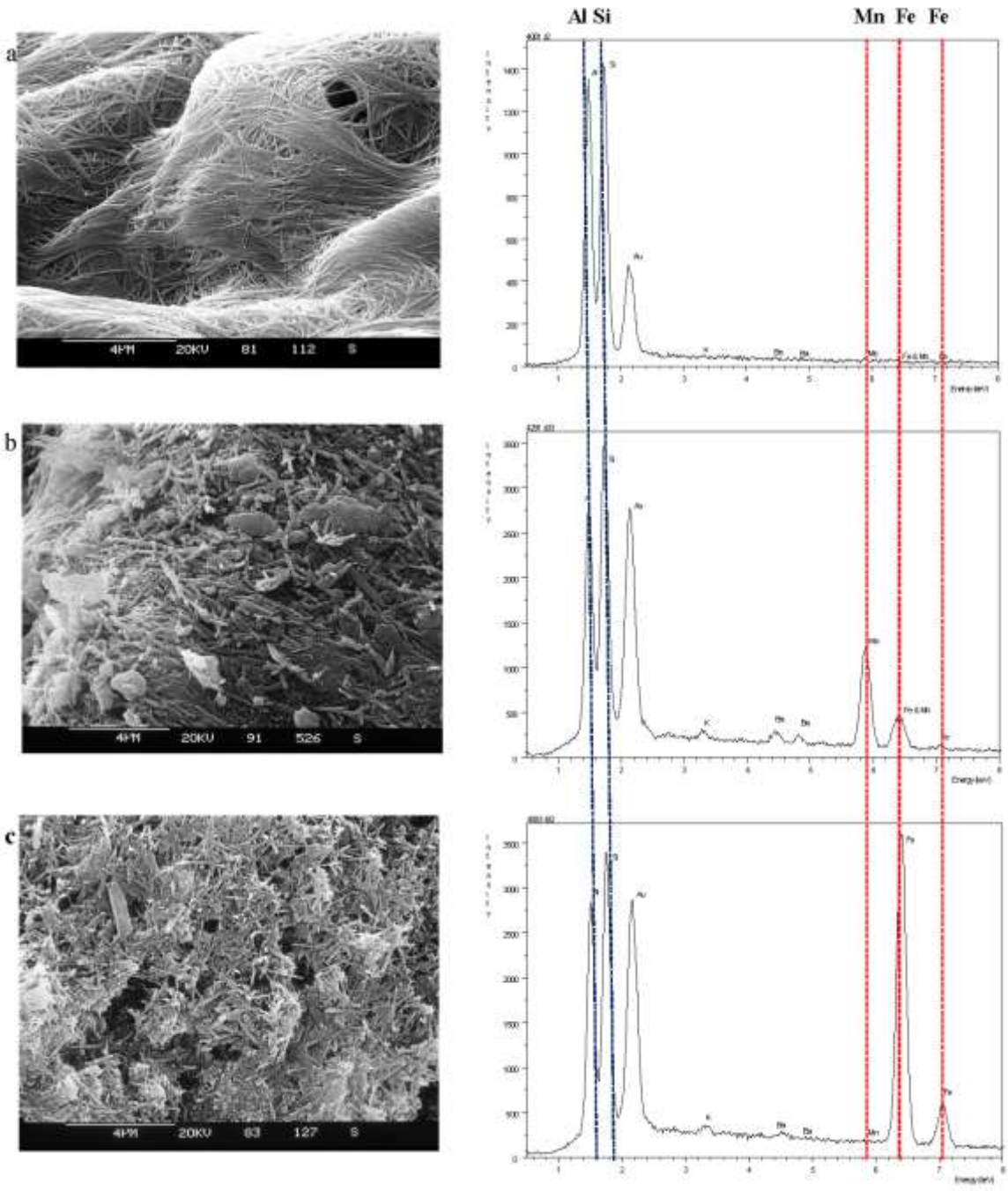

This is a 'pre-published' version of a paper accepted for publication in Clay Minerals.
This version may be changed during the production process.
The DOI, which may be used for citation purposes, but which will not be active until the version of record is published, is 10.1180/claymin.2016.051.3.14

Fig. 9

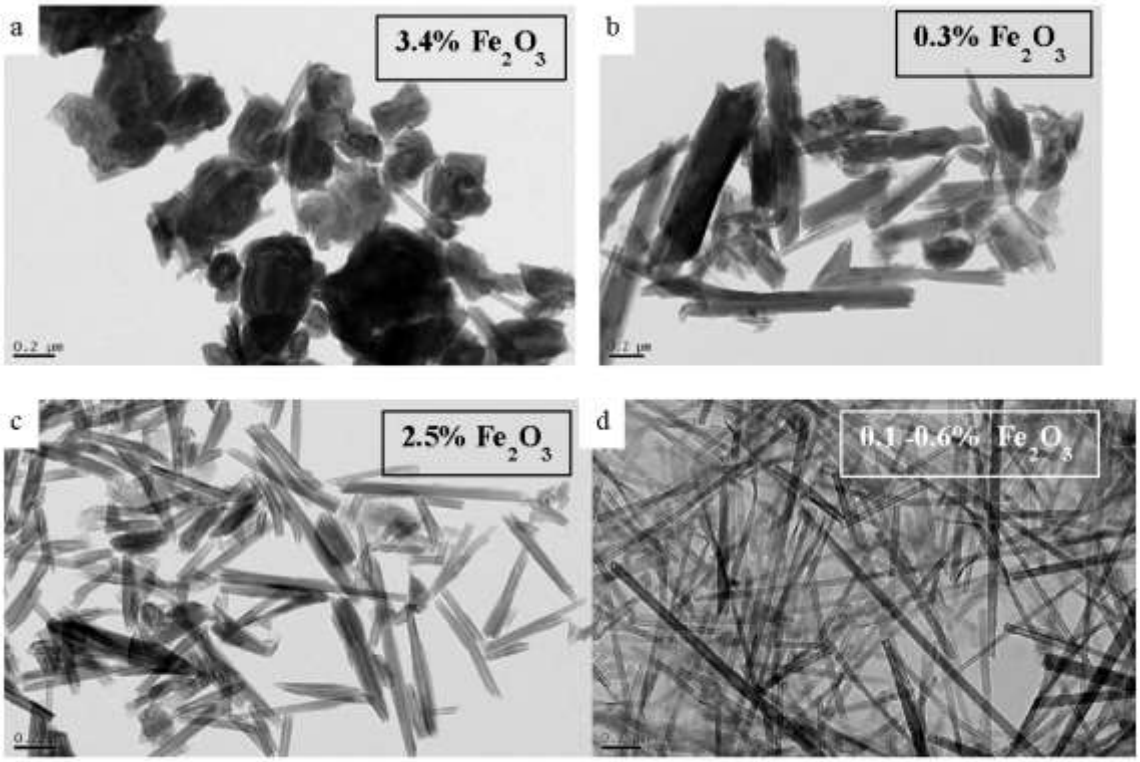

This is a 'pre-published' version of a paper accepted for publication in Clay Minerals.
This version may be changed during the production process.
The DOI, which may be used for citation purposes, but which will not be active until the version of record is published, is 10.1180/claymin.2016.051.3.14